Available online at www.sciencedirect.com
ScienceDirect
Deep-Sea Research II 54 (2007) 2208–2232
DEEP-SEA RESEARCH PART II
www.elsevier.com/locate/dsr2

# $^{234}$Th-derived particulate organic carbon export from an island-induced phytoplankton bloom in the Southern Ocean

Paul J. Morris[a,*], Richard Sanders[a], Robert Turnewitsch[a,1], Sandy Thomalla[b]

[a]National Oceanography Centre, University of Southampton, European Way, Southampton SO14 3ZH, UK
[b]Department of Oceanography, University of Cape Town, Private Bag, Rondebosch, Cape Town 7701, South Africa

Accepted 26 June 2007

**Abstract**

It has long been recognised that some oceanic regions have persistently low-chlorophyll levels, even though there are abundant inorganic nutrients. Studies have shown that these high-nutrient low-chlorophyll (HNLC) areas are depleted in iron, an essential micronutrient. In these regions biological production can be enhanced with artificial mesoscale iron fertilisation. However, the ability of iron-induced blooms to efficiently sequester carbon to mesopelagic depths is still an open question. It is hypothesised that sub-Antarctic islands in the HNLC Southern Ocean are also a source of iron and thus fuel the natural phytoplankton blooms observed in their proximity, thereby enhancing levels of particulate organic carbon (POC) export. To test the third part of this hypothesis, POC export was measured in the Southern Ocean region of the Crozet Islands (52°E, 46°S) during the austral summer of 2004/2005 as part of the CROZEX project. Based on satellite imagery, a high-chlorophyll region (maximum concentration = 4 μg l$^{-1}$) north and downstream of the islands was distinguished from a low-chlorophyll region (typical concentration = 0.3 μg l$^{-1}$) south and upstream of the islands. POC export estimates were obtained by using the naturally occurring particle-reactive radionuclide tracer $^{234}$Th. POC export was initially 15 mmol C m$^{-2}$ d$^{-1}$ in the high-chlorophyll bloom region, compared with 5 mmol C m$^{-2}$ d$^{-1}$ in the low-chlorophyll, non-bloom region. After a moderately small bloom at the southern control stations (max concentration = 0.7 μg l$^{-1}$) the spatial variability in POC export was lost, resulting in equally high levels of POC export (*ca.* 20 mmol C m$^{-2}$ d$^{-1}$) throughout the study region. Comparison of $^{234}$Th-derived POC export with estimates of new production, calculated from nitrate budgets, revealed evidence for a decoupling of new and export production, with this effect most apparent within the northern bloom area. In addition to methodological issues this apparent decoupling of new and export production could be due to a buildup of dissolved organic nitrogen within the bloom region, thus reducing the amount of POC available for export to mesopelagic depths.


*Keywords:* CROZEX; Crozet; Southern Ocean; $^{234}$Th; Carbon export; POC

## 1. Introduction

The role of the Southern Ocean in the global carbon cycle has come under increased scrutiny since the publication of the "iron hypothesis" by Martin (1990). Martin hypothesised that iron was a

*Corresponding author. Tel.: +44 23 8059 2012; fax: +44 23 8059 3052.
*E-mail address:* pjmorris@noc.soton.ac.uk (P.J. Morris).
[1]Present address: The Scottish Association for Marine Science, Dunstaffnage Marine Laboratory, Oban PA37 1QA, UK.

0967-0645/$ - see front matter © 2007 Elsevier Ltd. All rights reserved.
doi:10.1016/j.dsr2.2007.06.002

limiting micronutrient in high-nutrient low-chlorophyll (HNLC) ocean regions, and this has since been validated in various locations by artificial, *in situ* iron-fertilisation experiments (Martin et al., 1994; Coale et al., 1996, 2004; Boyd et al., 2000, 2004; Gervais et al., 2002; Tsuda et al., 2003; Hoffmann et al., 2006). The Southern Ocean is one such iron-limited HNLC area (Martin et al., 1990) and is of particular interest not only because it covers such a large area *ca.* $20 \times 10^6\,km^2$ (6% of total ocean area) but also because it has the potential to play a significant role in the global carbon cycle. Current estimates suggest that the Southern Ocean is responsible for the uptake of about $1\,Gt\,C\,yr^{-1}$ (Metzl et al., 1999), approximately 1% of the $90\,Gt\,C\,yr^{-1}$ taken up by the world's oceans annually (Prentice et al., 2001). However, models indicate that this figure has the potential to rise to 6–$30\,Gt\,C\,yr^{-1}$ given a scenario of complete nutrient utilisation supported by iron-replete conditions (Sarmiento and Orr, 1991).

The ability to induce phytoplankton blooms with the addition of iron raised hopes that it may be possible to sequester anthropogenic $CO_2$ in the deep ocean (Martin, 1990). By increasing phytoplankton productivity and the activity of the biological pump with the addition of iron, $CO_2$ could be drawn down from the atmosphere and therefore help reduce atmospheric $CO_2$ levels (Joos et al., 1991). However, determining whether iron fertilisation could be used to reduce atmospheric $CO_2$ has been an elusive question to answer (Zeebe and Archer, 2005, 2006; Chisholm et al., 2001; Johnson and Karl, 2002). Even though there remains continued discussion in the scientific literature as to whether iron fertilisation is a feasible strategy to sequester anthropogenic $CO_2$ (Buesseler and Boyd, 2003), the impetus and need to understand the effects of iron on phytoplankton productivity and the biological pump should be no less great.

To date, four iron-fertilisation experiments have been carried out in the Southern Ocean (Boyd et al., 2000; Gervais et al., 2002; Coale et al., 2004; Hoffmann et al., 2006), but the extent to which iron-induced blooms can sequester carbon to the deep ocean is still poorly constrained (Nodder et al., 2001; Charette and Buesseler, 2000; Buesseler et al., 2005; Bishop et al., 2004; Rutgers van der Loeff and Vöge, 2001). This is possibly because carbon export may continue to occur for some time period after the initial fertilisation by iron (Buesseler and Boyd, 2003; Buesseler et al., 2005), a time period that has been poorly sampled.

Artificial iron-fertilisation experiments have focussed on just the alleviation of iron limitation by adding iron in the form of $FeSO_4$. Although these elegant experiments have successfully shown the *in situ* link between iron enrichment and enhanced productivity, they are nonetheless simple perturbations of complex natural systems. Therefore, in addition to artificial iron-fertilisation experiments, recent years have seen efforts to try to understand the effects of natural iron fertilisation in HNLC regions. In natural fertilisation experiments the marine environment is probably influenced by a range of terrigeneous micronutrients. This contrasts with artificial iron-fertilisation experiments in which the concentration of only one micronutrient is changed. The challenge with natural fertilisation experiments will be to establish links between specific micronutrients and environmental responses to their injection.

The existence of large-scale blooms in the Southern Ocean tied to topographic features is clearly observable with satellite imagery (see Fig. 1 in Pollard et al., 2007a) and it is hypothesised that these blooms are sustained by a point source release of lithogenic iron into the surrounding waters. The most notable of these are austral summer blooms associated with South Georgia, Crozet and Kerguelen (Bucciarelli et al., 2001; Pollard et al., 2002; Korb and Whitehouse, 2004). Evidence supporting this hypothesis for the Kerguelen Islands and South Georgia has been reported by Blain et al. (2001, 2007) and Holeton et al. (2005), respectively. In studying these areas it may be possible to better understand the implications of iron fertilisation and thereby improve our ability to assess the response and efficiency of the biological pump to inputs of iron.

The focus of the CROZet natural iron bloom and EXport experiment (CROZEX) project is the annual bloom observed to the north of the Crozet Islands situated in the Indian sector of the Southern Ocean (Pollard and Sanders, 2006; Pollard et al., 2007b). Pollard et al. (2002) have hypothesised that this area is likely to be fertilised with iron from the plateau, giving rise to iron-replete conditions that induce a phytoplankton bloom in this otherwise HNLC region. The multidisciplinary CROZEX project aimed to survey the pervasive phytoplankton bloom to the north of the Crozet Islands and test the hypothesis that the islands and surrounding plateau are a source of bioavailable iron. In addition to an extensive physical hydrographic

survey to better constrain the circulation and flow of the Antarctic Circumpolar Current (ACC) in the region, a comprehensive set of biogeochemical observations was also made to categorise water-column chemistry, bloom ecology, and resultant carbon export.

In this study the radioactive particle tracer thorium-234 ($^{234}$Th, $t_{1/2} = 24.1$ d) (Bhat et al., 1969) was used to estimate how much photosynthetically fixed $CO_2$ was exported to mesopelagic depths as particulate organic carbon (POC) (Buesseler et al., 1992). $^{234}$Th is the daughter isotope of naturally occurring uranium-238 ($^{238}$U), which is conservative in seawater and proportional to salinity (Ku et al., 1977; Chen et al., 1986). Unlike $^{238}$U, $^{234}$Th is insoluble in seawater and adheres to particles in the water column. As particles sink through the water column, a radioactive disequilibrium is formed between $^{238}$U and $^{234}$Th, which can be used to quantify the rate of carbon export from the surface ocean when combined with data on the ratio of POC to particulate $^{234}$Th activity (Tsunogai and Minagawa, 1976).

The hypothesis is: Does a topographically associated bloom in the HNLC Southern Ocean export more POC to mesopelagic depths than non-bloom control sites.

## 2. Methods

### 2.1. Study area

The Crozet archipelago consists of five islands, on a plateau that covers an area of approximately 1200 × 600 km. The plateau rises from a surrounding abyssal depth of ≈3800 m to form a subsurface plateau 0–1000 m deep. The two major islands, Île de l'Est and Île de la Possession, are centred around 52°E and 46.4°S, approximately 2500 km southeast of Durban, South Africa. Île de l'Est and Île de la Possession reach maximum heights of 1090 and 934 m and cover areas of 130 and 150 km$^2$, respectively (Fig. 1). Their remoteness from any continental landmasses means they are ideally located for studying island effects in this HNLC region.

The Crozet Islands lie within the ACC, which has a generally eastward flow. As the ACC encounters the Del Caño Rise and the Crozet Plateau, it is forced to fragment with one filament pushed northwards and another filament skirting south of the topographic features. The northern filament moves north between the Del Caño Rise and the Crozet Plateau, turns west following constant depth topography, resulting in an anticyclonic flow, before finally turning east as part of the Crozet Front (Pollard and Read, 2001) (Fig. 2). It is believed that the northern branch of the ACC is a physical constraint on the spatial distribution of the Crozet bloom (Pollard et al., 2002). For a complete overview of the circulation around the Crozet archipelago, see Pollard et al. (2007b).

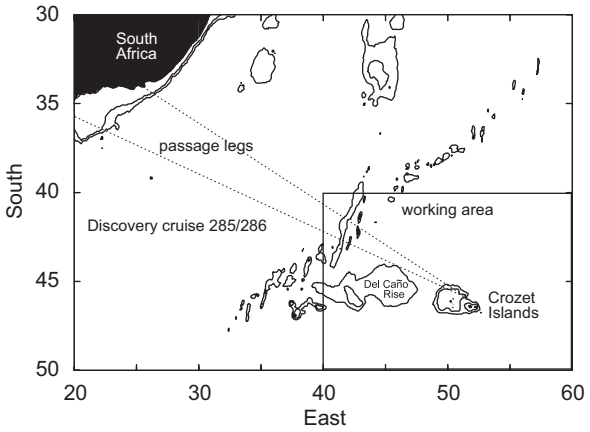


Fig. 1. Location of the Crozet Islands in the Indian sector of the Southern Ocean: 1000 m bathymetry contours are shown.

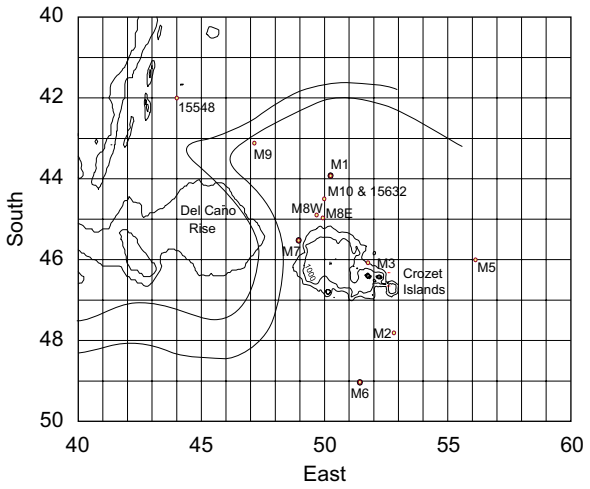


Fig. 2. Map of the CROZEX sampling area showing the major process stations: 1000 m bathymetry contours and the 'S' bend of the main branch of the Antarctic Circumpolar Current (ACC) are shown (Pollard et al., 2007b).

### 2.2. Sampling

Sampling for the CROZEX project took place from November 2004 to January 2005 on two

cruises onboard the R.R.S. *Discovery*, cruises D285 and D286, which will be referred to as leg 1 and leg 2, respectively, from hereon (Pollard and Sanders, 2006). Fig. 1 shows the study area and Fig. 2 shows the station locations. Sampling of discrete water samples was carried out with a 24-place sampling rosette with 20 L Niskin bottles and a CTD package. Samples for total $^{234}$Th were taken from 10 depths from 0 to $\approx$500 m, with the highest resolution in the top 200 m of the water column, and calibration samples were taken from 1000 m. Water samples were drawn into carboys rinsed with sample and were then transferred into the lab for total $^{234}$Th analysis.

### 2.3. Total $^{234}$Th analysis

The measurement of total (dissolved + particulate) $^{234}$Th activity in seawater samples was based on the $MnO_2$ precipitation method described by Rutgers van der Loeff and Moore (1999), similar to the procedures used by Turnewitsch and Springer (2001) and Thomalla et al. (2006). The procedure was scaled to use 10 L samples and all apparatus were washed with a solution of 10 ml of 30% $H_2O_2$ l$^{-1}$ in 1-l of 1 M HCl followed by rinsing with Milli-Q water.

To 10 L ($\pm$0.002 L) aliquots of each sample, three drops of 25% $NH_3$ and 125 μl of 60 g l$^{-1}$ $KMnO_4$ were added and mixed, followed by 50 μl of 400 g l$^{-1}$ $MnCl_2 \cdot 4H_2O$. After thoroughly mixing again, which produces a $MnO_2$ precipitate, the samples were allowed to stand for 8 h. The precipitate was resuspended and then filtered onto a 142 mm diameter (0.8 μm pore size), polycarbonate, Isopore filter, (Millipore product ATTP 142 50), ensuring all the solution passed through the filtration apparatus. Before departure for fieldwork the filters were checked for background activity in accordance with Rutgers van der Loeff and Moore (1999), and showed a combined filter and detector blank of $0.12 \pm 0.02$ cpm ($\bar{x} \pm 1\sigma$, $n = 8$). Following filtration, the filters were rinsed with 50 ml of Milli-Q water and drained of excess water under vacuum. While filters were still damp they were folded exactly in half and allowed to air dry. Once dry, filters were folded with repeatable geometry into $18 \times 18$ mm squares, wrapped in mylar film, and counted onboard ship on a low-level beta GM multicounter system (Model Risø GM-25-5A) for $^{234}$Th activity. Samples were counted as soon as possible after sampling with repeated counting over a 6-month period (>6 $^{234}$Th half-lives). This was to check that the activity decrease followed the decay of $^{234}$Th and also allowed a background correction for activity intrinsic to the detector and from other long-lived natural $\beta$-emitters. A regression analysis was carried out on the repeated counts to back calculate the $^{234}$Th activity to the time of sampling. All $^{234}$Th data are reported in units of disintegrations per minute per litre of seawater (dpm l$^{-1}$). Samples were counted to give a counting standard error of better than $\pm$3.5% (*ca.* $\geqslant$1000 counts) and the final activity of $^{234}$Th had a propagated error ranging from $\pm$5% to 10%.

To calibrate the total $^{234}$Th technique mid-water (1000 m) samples were used. These samples were collected well away from the surface ocean, coastal areas and seafloor nepheloid layers. Therefore, rates of processes other than radioactive production and decay of $^{234}$Th are negligible and $^{234}$Th is assumed to be in secular equilibrium with $^{238}$U (e.g., Bhat et al., 1969; Bacon et al., 1996; Bacon and Anderson, 1982; Charette and Moran, 1999; Buesseler et al., 2005; Rutgers van der Loeff et al., 1997, 2002, 2006; Bacon and Rutgers van der Loeff, 1989). As it is safe to assume radioactive equilibrium in mid-water samples, the $^{238}$U activity equals the total $^{234}$Th activity in these samples. Based on these known $^{234}$Th activities in mid-water samples counting efficiencies of $0.26 \pm 0.01$ and $0.28 \pm 0.01$ cpm dpm$^{-1}$ ($\bar{x} \pm 1\sigma$) were determined for legs 1 and 2, respectively. The likeliest explanation for this slight difference between these two sets of samples is that a different operator performed the total $^{234}$Th extractions and filter folding on each leg. Using the counting efficiencies for each leg and individual $^{238}$U and $^{234}$Th values for each sample, $^{234}$Th:$^{238}$U activity ratios at 1000 m were $1.00 \pm 0.02$ and $1.00 \pm 0.02$ ($\bar{x} \pm 1\sigma$, $n = 10$, $n = 9$) for legs 1 and 2, respectively. The corresponding reproducibility for total $^{234}$Th activities was $2.44 \pm 0.12$ dpm l$^{-1}$ (4.9%) and $2.46 \pm 0.08$ dpm l$^{-1}$ (3.3%) ($\bar{x} \pm 1\sigma$, $n = 10$, $n = 9$) for legs 1 and 2, respectively. $^{238}$U is conservative in oxygenated seawater and can therefore be calculated from salinity (Chen et al., 1986; Delanghe et al., 2002; Ku et al., 1977; Rutgers van der Loeff et al., 2006). $^{238}$U activities ($A_u$, dpm kg$^{-1}$) were calculated from the relationship published by Chen et al. (1986), where $A_u = 0.0686 \times$ salinity, based on the average uranium concentration in seawater of 3.238 ng g$^{-1}$ normalised to a salinity of 35. The uncertainty in the $^{238}$U–salinity relationship was estimated to be 3.3%, an average of linear

regression errors at the 68.3% ($1\sigma$) and 95.4% ($2\sigma$) confidence levels in the data by Chen et al. (1986). Traditionally the $1\sigma$ uncertainty of the Chen et al. (1986) data set has been used as a representative uncertainty of $^{238}$U activities. However, since the work of Chen et al. (1986) more data have been added to the $^{238}$U–salinity relationship (see, e.g., compilations in Rutgers van der Loeff et al., 2006; Speicher et al., 2006). Given the evolving shape of the $^{238}$U–salinity data set we believe an uncertainty of $\approx$3.3% is more representative than the $1\sigma$ uncertainty in the Chen et al. (1986) data set usually used. The extraction efficiency of $^{234}$Th from seawater samples was estimated by re-precipitating a number of samples for a second time. The extraction efficiencies were $98\pm3\%$ and $99\pm3\%$ ($\bar{x}\pm1\sigma$, $n=10$, $n=8$) for legs 1 and 2, respectively, and were therefore not considered to be significantly different from 100% extraction efficiency. These extraction efficiencies compare well with the efficiencies reported by Rutgers van der Loeff and Moore (1999) and Turnewitsch and Springer (2001). The *in situ* activity per unit volume of water was calculated based on the *in situ* density.

### 2.4. $^{234}$Th export model description

The rate of $^{234}$Th export out of the surface ocean was calculated using a steady state (SS) scavenging model (Coale and Bruland, 1985, 1987; Buesseler et al., 1992; Cochran et al., 1995, 2000). In a given parcel of water, the total (dissolved + particulate) activity of $^{234}$Th is controlled by several processes: ingrowth from $^{238}$U, radioactive decay, loss on settling particles, and advection and turbulent diffusion. These processes can be expressed as

$$\frac{\partial A_t}{\partial t} = \left[A_U - (A_p + A_d)\right]\lambda - P + V, \quad (1)$$

where $\partial A_t/\partial t$ (dpm m$^{-3}$ d$^{-1}$) is the rate of change in total $^{234}$Th activity (dpm m$^{-3}$), $A_U$ is the $^{238}$U activity (dpm m$^{-3}$), $A_p$ and $A_d$ are the particulate and dissolved $^{234}$Th activities, respectively (dpm m$^{-3}$) (the sum of which is $A_t$ the total $^{234}$Th activity (dpm m$^{-3}$)), $\lambda$ is the decay constant of $^{234}$Th (d$^{-1}$), $P$ is the loss of $^{234}$Th activity on sinking particles (dpm m$^{-3}$ d$^{-1}$), and $V$ is the sum of advective and turbulent diffusive $^{234}$Th activity fluxes into and out of the parcel of water (dpm m$^{-3}$ d$^{-1}$). $P$ is the term of interest when calculating particle flux so Eq. (1) can be rearranged to give

$$P = (A_U - A_t)\lambda - \frac{\partial A_t}{\partial t} + V. \quad (2)$$

By integrating Eq. (2) by depth intervals through the water column it is then possible to calculate the flux of $^{234}$Th through any depth horizon that has been sampled. By treating every station as a separate profile, thus assuming SS conditions ($\partial A_t/\partial t = 0$) and assuming $V = 0$, Eq. (2) can be simplified to give

$$P = \int_0^z \lambda(A_U - A_t)\,dz. \quad (3)$$

The term $V$ comprises of processes such as horizontal and vertical advection and horizontal and vertical turbulent diffusion. These processes are associated with gradients in the $^{234}$Th distribution and have an impact on $^{234}$Th budget calculations. It has been shown that horizontal advection, upwelling (vertical advection) and horizontal turbulent diffusion can be significant in upwelling regions such as the equatorial Pacific at 140°W and the northwestern Arabian Sea (Buesseler et al., 1995, 1998; Bacon et al., 1996; Dunne and Murray, 1999), and in coastal areas where enhanced particle scavenging in shallower water columns is often seen (e.g., Gustafsson et al., 1998). How valid is the assumption that $V = 0$ in this study?

Most sampling sites of the CROZEX process study (M1, M2, M5, M6, M7, M8, M10, 15632) were located away from regions that could be associated with major vertical advective current velocities. The Polar Frontal Zone (PFZ), at which cold Antarctic water is subducted beneath warm subtropical water (Deacon, 1984), is typically located $>100$ km from our sampling sites based on the flow on the northern branch of the ACC (Fig. 2). Thus, even if some water from the sampling sites should be entrained by the downwelling typical of the PFZ, it would probably still be a rather horizontal water movement at the sampling sites. Deeper water has to flow around the Crozet Plateau and this movement may involve vertical advective flow. However, this vertical flow component is likely to occur mainly in the vicinity of the plateau. Only the topmost few hundred metres of the water column was sampled while total water depths were $\geqslant$2000 m, and horizontal distances to the slope and shallow parts of the plateau were at least several tens of kilometres. Therefore, it seems to be relatively safe to assume that large-scale topographically

related vertical advective flow did not play an important role in controlling the $^{234}$Th distribution at our sampling sites.

At M3, the assumption that vertical turbulent diffusive fluxes were negligible could be directly scrutinised with measured vertical turbulent diffusion coefficients ($K_z$). $K_z$ at M3 was estimated by two methods: with LADCP data (Naveira Garabato et al., 2004) and with radium-228 ($^{228}$Ra) data (Moore, 2000). LADCP results gave a $K_z$ in the upper 50–300 m of the water column of 0.34–0.41 $cm^2 s^{-1}$, whereas $^{228}$Ra data gave much higher rates of 11–100 $cm^2 s^{-1}$ (Charette et al., 2007), thus presenting a very large range. Charette et al. (2007) suggest that the reasons for the much higher $^{228}$Ra-derived values for $K_z$ may result from (1) the highly dynamic nature of the surface ocean over seasonal time-scales, (2) that the $^{228}$Ra method integrates over a much longer time period, and (3) the $^{228}$Ra 1-D model approach for estimating $K_z$ may be influenced by horizontal advection. Therefore, the LADCP-derived $K_z$ values were considered to be more representative of vertical diffusion across the base of the mixed layer. The LADCP-derived $K_z$ at M3 agrees well with estimates of $K_z$ measured in the Southern Ocean during SOIREE of 0.3 $cm^2 s^{-1}$ (Law et al., 2003). Therefore, to put a reasonable upper limit on the flux of $^{234}$Th activity being brought into the surface ocean through vertical turbulent diffusion, a value of 1 $cm^2 s^{-1}$ was applied to the $^{234}$Th gradient across the bottom depth horizon of $^{234}$Th/$^{238}$U. The turbulent diffusive flux of $^{234}$Th, $V_z$ (dpm $m^{-2} d^{-1}$), across this layer was calculated using

$$V_z = K_z\left(\frac{\partial^{234}\mathrm{Th}}{\partial z}\right), \tag{4}$$

where $K_z$ is the vertical diffusion coefficient ($cm^2 s^{-1}$) and $\partial^{234}$Th/$\partial z$ is the $^{234}$Th activity gradient across the bottom depth horizon of $^{234}$Th/$^{238}$U disequilibrium. At M3, the upward vertical turbulent diffusive flux of $^{234}$Th was estimated to be in the range of 2–52 dpm $m^{-2} d^{-1}$, less than 3% of particle-associated downward fluxes in all cases, which is within the overall uncertainty of $^{234}$Th export estimates. Based on a combination of this information it was assumed that vertical turbulent diffusion was negligible throughout the study region.

Horizontal advection and diffusion were also considered to be minimal because the residence time of water in the region is about 62 days (Pollard et al., 2007b), which is about three times the half-life of $^{234}$Th. In addition to this the profiles of $^{234}$Th were reasonably consistent between stations therefore limiting horizontal gradients in $^{234}$Th and resultant lateral net flux. Based on these results it seems reasonably safe to assume that no significant horizontal and vertical advection and horizontal and vertical turbulent diffusion were having an impact on the $^{234}$Th distribution at our sampling sites. Therefore, a model without advection and turbulent diffusion term $V$ was applied to individual total $^{234}$Th profiles to give $^{234}$Th flux estimates out of the surface ocean and into the deep ocean (cf., Tanaka et al., 1983; Wei and Murray, 1991; Moran and Buesseler, 1993).

The SS model is a useful approach because it requires only one profile of $^{234}$Th activities to calculate a $^{234}$Th flux. However, if multiple profiles of $^{234}$Th activities are collected from the same site over a period of time then a NSS model can be applied. It has been shown that a non-steady state (NSS) model is more suitable during high particle export events, for example during a plankton bloom onset and termination (Buesseler et al., 1992; Buesseler, 1998; Cochran et al., 1995, 1997; Savoye et al., 2006). However, a NSS approach requires multiple observations of the same parcel of water. An initial analysis using the SS model was applied to all the stations individually and then a NSS model was applied to selected stations. During the cruise, four locations were sampled more than once: M2 and M6 to the south of the Crozet plateau, M9 in the NW of the study region and M3 the time-series station (Fig. 2). The NSS model factors in the term $\partial A_t/\partial t$, which was originally made to equal zero in the SS model. The advective and turbulent diffusive term $V$ was still made to equal zero for the reasons previously discussed. Therefore, the NSS model for the calculation of $^{234}$Th export across a depth horizon $z$ can be represented by

$$P = \int_0^z \lambda(A_U - A_t) - \frac{\partial A_t}{\partial t}\,\mathrm{d}z. \tag{5}$$

By calculating $\partial A_t/\partial t$ a NSS $^{234}$Th flux was calculated for M2, M6, and M9. M3 will be discussed separately due to its unique situation.

### 2.5. Carbon-to-thorium (C:Th) ratio

To estimate POC export, the ratio of POC to particulate $^{234}$Th activity (C:Th μmol dpm$^{-1}$) has to be applied to the measured $^{234}$Th export fluxes.

Although the abundance of particles fall into the smaller size classes, it is thought that the larger particles dominate particle export (Fowler and Knauer, 1986), with the larger size class (>53 μm) considered to represent the bulk of particulates rapidly settling through the water column (Bishop et al., 1977). To sample adequately the rarer large particles, large sample volumes must be filtered to allow enough material to be collected for analysis, with *in situ* filter pumps typically the method of choice (Buesseler et al., 2006). Therefore, every time a profile for total $^{234}$Th was taken, particles were collected by filtering large volumes of seawater through a 293 mm diameter, 50 μm nylon mesh. High-volume filtration was carried out with an *in situ* stand-alone pump system (SAPS; Challenger Oceanic) deployed approximately 20 m below the mixed layer. The depth of the mixed layer was deduced from a combination of temperature, fluorescence and transmittance data collected in real time from the CTD package. Once on board, the particles were rinsed off the mesh and re-suspended with "thorium-free-seawater" (which is the filtrate remaining after particulate and $MnO_2$ extraction). The suspension was split using a Folsom sample splitter so that POC and $^{234}$Th could be quantitatively measured on the same sample. One split was filtered onto a pre-combusted, pre-weighed, 25 mm diameter, GFF filter and stored at −20 °C for POC/nitrogen (N) analyses. POC/N samples were analysed with the high-temperature combustion technique with acetanilide as a standard. A good account of POC/N analysis is given by Ehrhardt and Koeve (1999). The second split was filtered for $^{234}$Th analysis onto a 142 mm diameter (0.8 μm pore size), polycarbonate, Isopore filter, (Millipore product ATTP 142 50), ensuring all the particles passed through the filtration apparatus. These filters were prepared for beta counting in the same way as that described for total $^{234}$Th and were calibrated using the total $^{234}$Th counting efficiency. The C:Th ratios were then applied to the $^{234}$Th fluxes according to equation:

$$\text{POC flux} = \text{C} : \text{Th} \times P, \tag{6}$$

where POC flux is the quantity of POC (μmol m$^{-2}$ d$^{-1}$) falling out the surface ocean, C:Th is the ratio of POC to $^{234}$Th (μmol dpm$^{-1}$) on the large size class of particles (>50 μm), and $P$ is the integrated $^{234}$Th flux (dpm m$^{-2}$ d$^{-1}$) derived from Eqs. (3) and (5). This procedure was first demonstrated by Tsunogai and Minagawa (1976), but was not routinely used until the concept was again highlighted by Buesseler et al. (1992). This same approach can be used to calculate fluxes of other elements such as nitrogen and silica by calculating ratios between $^{234}$Th and particulate organic nitrogen (PON) and biogenic silica, respectively.

## 3. Results

### 3.1. General synopsis

During the sampling period, a total of 20 process stations were occupied (Pollard and Sanders, 2006) (Fig. 2, Table 1) and sampled for $^{234}$Th. Ten stations were sampled on each of leg 1 and leg 2. Of the 20 stations sampled for $^{234}$Th, six were repeat occupation of three locations (M2, M6, and M9), eight were repeat occupations of M3, and six were single profile stations. Station M3 was located 38 km north of Île de la Possession and was deemed a time-series station to make repeated observations in an area, which usually sustains a bloom throughout the bloom season. The locations of Stations M2 and M6 were picked for their non-bloom characteristics to act as control, stations. Repeat occupations of the same location are denoted by decimals, e.g., M3.1 and M3.2 are the first and second occupations of M3, respectively.

As with previous years, an intense bloom was observed to the north of the islands with chlorophyll levels peaking at 4 μg l$^{-1}$ at the start of November. To the south of the islands, no such bloom was observed, again consistent with previous years, although at the start of December a small increase in surface chlorophyll up to 0.7 μg l$^{-1}$ was observed. Typical chlorophyll levels prior to the bloom development were ≈0.3 μg l$^{-1}$ throughout the study area. For details of the bloom progression see Figs. 3 and 5 in Venables et al. (2007). An interesting feature near this location was the appearance of a small, secondary, eddy bloom (Allen et al., 2006) that persisted after the main widespread bloom had declined. The eddy had chlorophyll levels of 6 μg l$^{-1}$, the highest observed during both legs.

### 3.2. $^{234}$Th disequilibria

The complete data set of total $^{234}$Th, $^{238}$U (dpm l$^{-1}$) and associated $^{234}$Th:$^{238}$U ratios for all stations and all depths is given in Table 1. A $^{234}$Th:$^{238}$U ratio of <1 in a given parcel of water

Table 1
Total $^{234}$Th and $^{238}$U activities (dpm l$^{-1}$), and $^{234}$Th:$^{238}$U activity ratios with 1$\sigma$ errors for all stations

| Station name and number | Date (dd/mm/yy) | Depth (m) | Total $^{234}$Th (dpm l$^{-1}$) | $^{238}$U (dpm l$^{-1}$) | $^{234}$Th:$^{238}$U |
|---|---|---|---|---|---|
| 15492-M1 | 38301 | 12 | 1.40±0.07 | 2.38±0.08 | 0.59±0.04 |
| | | 17 | 1.51±0.10 | 2.38±0.08 | 0.64±0.05 |
| | | 26 | 1.43±0.07 | 2.38±0.08 | 0.60±0.04 |
| | | 46 | 1.36±0.07 | 2.38±0.08 | 0.57±0.04 |
| | | 66 | 1.59±0.08 | 2.38±0.08 | 0.67±0.04 |
| | | 87 | 1.97±0.10 | 2.38±0.08 | 0.83±0.05 |
| | | 117 | 2.67±0.16 | 2.39±0.08 | 1.12±0.08 |
| | | 158 | 2.39±0.17 | 2.39±0.08 | 1.00±0.08 |
| | | 209 | 2.41±0.13 | 2.40±0.08 | 1.00±0.06 |
| | | 1014 | 2.66±0.14 | 2.45±0.08 | 1.08±0.07 |
| 15495-M3.1 | 38303 | 6 | 1.68±0.08 | 2.38±0.08 | 0.70±0.04 |
| | | 41 | 1.90±0.10 | 2.38±0.08 | 0.80±0.05 |
| | | 77 | 1.80±0.09 | 2.39±0.08 | 0.75±0.05 |
| | | 126 | 2.05±0.10 | 2.39±0.08 | 0.86±0.05 |
| | | 153 | 2.63±0.13 | 2.39±0.08 | 1.10±0.07 |
| | | 203 | 2.19±0.13 | 2.39±0.08 | 0.91±0.06 |
| | | 228 | 2.18±0.11 | 2.39±0.08 | 0.91±0.05 |
| | | 254 | 2.56±0.13 | 2.40±0.08 | 1.07±0.06 |
| | | 304 | 2.48±0.12 | 2.40±0.08 | 1.03±0.06 |
| | | 1010 | 2.72±0.13 | 2.45±0.08 | 1.11±0.07 |
| 15498-M3.2 | 38308 | 13 | 2.01±0.14 | 2.39±0.08 | 0.84±0.07 |
| | | 44 | 2.06±0.10 | 2.39±0.08 | 0.86±0.05 |
| | | 63 | 2.07±0.10 | 2.39±0.08 | 0.87±0.05 |
| | | 83 | 2.20±0.11 | 2.39±0.08 | 0.92±0.05 |
| | | 103 | 2.48±0.16 | 2.39±0.08 | 1.04±0.08 |
| | | 128 | 2.23±0.11 | 2.39±0.08 | 0.93±0.06 |
| | | 154 | 2.32±0.11 | 2.40±0.08 | 0.97±0.06 |
| | | 179 | 2.27±0.13 | 2.40±0.08 | 0.95±0.06 |
| | | 206 | 2.37±0.13 | 2.40±0.08 | 0.99±0.06 |
| | | 304 | 2.70±0.15 | 2.41±0.08 | 1.12±0.07 |
| 15503-M2.1 | 38310 | 12 | 2.05±0.10 | 2.38±0.08 | 0.86±0.05 |
| | | 42 | 2.25±0.13 | 2.38±0.08 | 0.94±0.06 |
| | | 63 | 2.18±0.11 | 2.38±0.08 | 0.91±0.05 |
| | | 83 | 2.11±0.10 | 2.38±0.08 | 0.88±0.05 |
| | | 128 | 2.40±0.12 | 2.39±0.08 | 1.00±0.06 |
| | | 153 | 2.36±0.14 | 2.39±0.08 | 0.99±0.07 |
| | | 178 | 2.50±0.13 | 2.39±0.08 | 1.04±0.06 |
| | | 254 | 2.43±0.12 | 2.40±0.08 | 1.01±0.06 |
| | | 381 | 2.48±0.12 | 2.42±0.08 | 1.03±0.06 |
| | | 506 | 2.53±0.13 | 2.43±0.08 | 1.04±0.06 |
| 15512-M6.1 | 38313 | 12 | 2.05±0.10 | 2.38±0.08 | 0.86±0.05 |
| | | 42 | 2.21±0.18 | 2.38±0.08 | 0.93±0.08 |
| | | 62 | 2.25±0.11 | 2.38±0.08 | 0.94±0.06 |
| | | 83 | 2.18±0.12 | 2.38±0.08 | 0.91±0.06 |
| | | 104 | 2.42±0.12 | 2.38±0.08 | 1.01±0.06 |
| | | 126 | 2.20±0.13 | 2.39±0.08 | 0.92±0.06 |
| | | 154 | 2.33±0.11 | 2.39±0.08 | 0.98±0.06 |
| | | 177 | 2.25±0.12 | 2.39±0.08 | 0.94±0.06 |
| | | 204 | 2.42±0.12 | 2.39±0.08 | 1.01±0.06 |
| | | 507 | 2.66±0.13 | 2.43±0.08 | 1.10±0.07 |
| 15517-M3.3 | 38315 | 14 | 1.77±0.09 | 2.39±0.08 | 0.74±0.04 |
| | | 44 | 1.83±0.15 | 2.39±0.08 | 0.76±0.07 |
| | | 65 | 1.78±0.09 | 2.39±0.08 | 0.74±0.04 |

Table 1 (*continued*)

| Station name and number | Date (dd/mm/yy) | Depth (m) | Total $^{234}$Th (dpm l$^{-1}$) | $^{238}$U (dpm l$^{-1}$) | $^{234}$Th:$^{238}$U |
|---|---|---|---|---|---|
| | | 85 | 1.82±0.09 | 2.39±0.08 | 0.76±0.05 |
| | | 105 | 2.16±0.11 | 2.39±0.08 | 0.90±0.05 |
| | | 130 | 2.14±0.11 | 2.39±0.08 | 0.90±0.05 |
| | | 156 | 2.33±0.12 | 2.39±0.08 | 0.97±0.06 |
| | | 179 | 2.42±0.13 | 2.39±0.08 | 1.01±0.06 |
| | | 205 | 2.37±0.12 | 2.40±0.08 | 0.99±0.06 |
| | | 307 | 2.54±0.13 | 2.41±0.08 | 1.05±0.07 |
| 15523-M7 | 38317 | 12 | 1.35±0.07 | 2.38±0.08 | 0.56±0.03 |
| | | 43 | 1.47±0.13 | 2.38±0.08 | 0.62±0.06 |
| | | 63 | 1.47±0.08 | 2.38±0.08 | 0.62±0.04 |
| | | 84 | 1.69±0.09 | 2.39±0.08 | 0.71±0.04 |
| | | 103 | 2.17±0.11 | 2.39±0.08 | 0.91±0.05 |
| | | 129 | 2.43±0.13 | 2.39±0.08 | 1.01±0.06 |
| | | 153 | 2.66±0.13 | 2.39±0.08 | 1.11±0.07 |
| | | 179 | 2.39±0.12 | 2.40±0.08 | 1.00±0.06 |
| | | 204 | 2.36±0.14 | 2.40±0.08 | 0.98±0.07 |
| | | 302 | 2.64±0.13 | 2.41±0.08 | 1.09±0.06 |
| 15533-M8E | 38320 | 12 | 1.56±0.10 | 2.38±0.08 | 0.66±0.05 |
| | | 43 | 1.75±0.13 | 2.38±0.08 | 0.74±0.06 |
| | | 63 | 1.84±0.10 | 2.38±0.08 | 0.77±0.05 |
| | | 82 | 1.95±0.11 | 2.38±0.08 | 0.82±0.05 |
| | | 101 | 2.47±0.13 | 2.39±0.08 | 1.04±0.06 |
| | | 126 | 2.43±0.14 | 2.39±0.08 | 1.02±0.07 |
| | | 153 | 2.45±0.13 | 2.39±0.08 | 1.03±0.06 |
| | | 179 | 2.46±0.13 | 2.40±0.08 | 1.03±0.06 |
| | | 204 | 2.44±0.14 | 2.40±0.08 | 1.02±0.07 |
| | | 405 | 2.55±0.13 | 2.42±0.08 | 1.06±0.06 |
| 15539-M8W | 38322 | 10 | 1.36±0.07 | 2.39±0.08 | 0.57±0.04 |
| | | 41 | 1.50±0.08 | 2.39±0.08 | 0.63±0.04 |
| | | 62 | 1.66±0.11 | 2.39±0.08 | 0.69±0.05 |
| | | 81 | 1.80±0.09 | 2.39±0.08 | 0.75±0.04 |
| | | 103 | 2.24±0.12 | 2.39±0.08 | 0.93±0.06 |
| | | 127 | 2.23±0.14 | 2.39±0.08 | 0.93±0.06 |
| | | 152 | 2.47±0.13 | 2.39±0.08 | 1.03±0.06 |
| | | 177 | 2.35±0.12 | 2.40±0.08 | 0.98±0.06 |
| | | 205 | 2.33±0.12 | 2.40±0.08 | 0.97±0.06 |
| | | 404 | 2.54±0.21 | 2.41±0.08 | 1.05±0.09 |
| 15542-M9.1 | 38323 | 10 | 0.94±0.05 | 2.38±0.08 | 0.39±0.03 |
| | | 41 | 1.31±0.08 | 2.38±0.08 | 0.55±0.04 |
| | | 61 | 1.93±0.09 | 2.39±0.08 | 0.81±0.05 |
| | | 81 | 2.31±0.14 | 2.39±0.08 | 0.97±0.07 |
| | | 101 | 2.55±0.14 | 2.39±0.08 | 1.06±0.07 |
| | | 121 | 2.36±0.12 | 2.40±0.08 | 0.99±0.06 |
| | | 122 | 2.38±0.13 | 2.40±0.08 | 0.99±0.06 |
| | | 122 | 2.31±0.13 | 2.40±0.08 | 0.96±0.06 |
| | | 203 | 2.44±0.23 | 2.40±0.08 | 1.02±0.10 |
| | | 404 | 2.63±0.18 | 2.41±0.08 | 1.09±0.08 |
| 15548 | 38325 | 1004 | 2.46±0.14 | 2.44±0.08 | 1.01±0.07 |
| | | 1003 | 2.51±0.19 | 2.44±0.08 | 1.03±0.09 |
| | | 1003 | 2.47±0.16 | 2.44±0.08 | 1.01±0.07 |
| | | 1004 | 2.39±0.12 | 2.44±0.08 | 0.98±0.06 |
| | | 1002 | 2.59±0.14 | 2.44±0.08 | 1.06±0.07 |
| | | 1005 | 2.22±0.11 | 2.44±0.08 | 0.91±0.05 |
| | | 1005 | 2.27±0.11 | 2.44±0.08 | 0.93±0.06 |

Table 1 (*continued*)

| Station name and number | Date (dd/mm/yy) | Depth (m) | Total $^{234}$Th (dpm l$^{-1}$) | $^{238}$U (dpm l$^{-1}$) | $^{234}$Th:$^{238}$U |
|---|---|---|---|---|---|
| | | 1003 | 2.54±0.15 | 2.44±0.08 | 1.04±0.07 |
| | | 1004 | 2.42±0.16 | 2.44±0.08 | 0.99±0.07 |
| | | 1005 | 2.54±0.18 | 2.44±0.08 | 1.04±0.08 |
| 15554-M9.2 | 38339 | 11 | 1.43±0.13 | 2.38±0.08 | 0.60±0.06 |
| | | 26 | 1.58±0.15 | 2.38±0.08 | 0.66±0.07 |
| | | 52 | 1.54±0.09 | 2.39±0.08 | 0.65±0.04 |
| | | 77 | 1.71±0.06 | 2.39±0.08 | 0.72±0.03 |
| | | 102 | 2.09±0.08 | 2.39±0.08 | 0.87±0.04 |
| | | 120 | 1.89±0.07 | 2.40±0.08 | 0.79±0.04 |
| | | 150 | 2.17±0.08 | 2.40±0.08 | 0.91±0.04 |
| | | 175 | 2.30±0.18 | 2.40±0.08 | 0.96±0.08 |
| | | 200 | 2.16±0.08 | 2.40±0.08 | 0.90±0.04 |
| | | 405 | 2.41±0.08 | 2.41±0.08 | 1.00±0.05 |
| 15560-M10 | 38340 | 12 | 1.62±0.09 | 2.38±0.08 | 0.68±0.04 |
| | | 22 | 1.72±0.06 | 2.38±0.08 | 0.72±0.03 |
| | | 42 | 1.71±0.07 | 2.38±0.08 | 0.72±0.04 |
| | | 62 | 1.81±0.08 | 2.38±0.08 | 0.76±0.04 |
| | | 81 | 2.08±0.17 | 2.38±0.08 | 0.87±0.08 |
| | | 112 | 2.20±0.10 | 2.39±0.08 | 0.92±0.05 |
| | | 152 | 2.44±0.18 | 2.39±0.08 | 1.02±0.08 |
| | | 178 | 2.39±0.09 | 2.39±0.08 | 1.00±0.05 |
| | | 203 | 2.31±0.08 | 2.40±0.08 | 0.96±0.05 |
| | | 404 | 2.61±0.18 | 2.42±0.08 | 1.08±0.08 |
| 15574-M3.4 | 38343 | 12 | 1.63±0.06 | 2.38±0.08 | 0.68±0.03 |
| | | 23 | 1.77±0.14 | 2.38±0.08 | 0.74±0.06 |
| | | 52 | 1.61±0.07 | 2.38±0.08 | 0.67±0.04 |
| | | 73 | 1.66±0.07 | 2.39±0.08 | 0.70±0.04 |
| | | 103 | 2.03±0.09 | 2.39±0.08 | 0.85±0.05 |
| | | 133 | 2.11±0.09 | 2.39±0.08 | 0.88±0.05 |
| | | 154 | 2.23±0.09 | 2.39±0.08 | 0.93±0.05 |
| | | 184 | 2.23±0.10 | 2.40±0.08 | 0.93±0.05 |
| | | 305 | 2.33±0.11 | 2.41±0.08 | 0.97±0.06 |
| | | 409 | 2.45±0.10 | 2.42±0.08 | 1.02±0.05 |
| 15580-M5 | 38347 | 13 | 1.63±0.16 | 2.38±0.08 | 0.69±0.07 |
| | | 22 | 1.60±0.05 | 2.38±0.08 | 0.67±0.03 |
| | | 52 | 1.69±0.15 | 2.38±0.08 | 0.71±0.07 |
| | | 72 | 1.67±0.08 | 2.38±0.08 | 0.70±0.04 |
| | | 103 | 1.85±0.06 | 2.38±0.08 | 0.78±0.04 |
| | | 128 | 1.95±0.06 | 2.38±0.08 | 0.82±0.04 |
| | | 154 | 2.17±0.10 | 2.39±0.08 | 0.91±0.05 |
| | | 203 | 2.33±0.14 | 2.39±0.08 | 0.98±0.07 |
| | | 304 | 2.28±0.12 | 2.41±0.08 | 0.95±0.06 |
| | | 508 | 2.64±0.10 | 2.43±0.08 | 1.09±0.05 |
| 15590-M3.5 | 38351 | 12 | 1.71±0.11 | 2.39±0.08 | 0.72±0.05 |
| | | 22 | 1.75±0.07 | 2.39±0.08 | 0.73±0.04 |
| | | 53 | 1.81±0.16 | 2.39±0.08 | 0.76±0.07 |
| | | 72 | 1.87±0.06 | 2.39±0.08 | 0.78±0.04 |
| | | 104 | 2.13±0.09 | 2.39±0.08 | 0.89±0.05 |
| | | 129 | 2.08±0.07 | 2.40±0.08 | 0.87±0.04 |
| | | 155 | 2.13±0.08 | 2.40±0.08 | 0.89±0.04 |
| | | 204 | 2.32±0.22 | 2.40±0.08 | 0.97±0.10 |
| | | 305 | 2.37±0.20 | 2.41±0.08 | 0.98±0.09 |
| | | 507 | 2.40±0.11 | 2.42±0.08 | 0.99±0.06 |

Table 1 (*continued*)

| Station name and number | Date (dd/mm/yy) | Depth (m) | Total $^{234}$Th (dpm l$^{-1}$) | $^{238}$U (dpm l$^{-1}$) | $^{234}$Th:$^{238}$U |
|---|---|---|---|---|---|
| 15595-M6.2 | 38354 | 13 | 1.65±0.07 | 2.38±0.08 | 0.69±0.04 |
| | | 43 | 1.86±0.17 | 2.38±0.08 | 0.78±0.08 |
| | | 72 | 1.78±0.07 | 2.38±0.08 | 0.75±0.04 |
| | | 104 | 1.73±0.06 | 2.39±0.08 | 0.73±0.03 |
| | | 122 | 1.99±0.08 | 2.39±0.08 | 0.83±0.04 |
| | | 144 | 2.31±0.08 | 2.39±0.08 | 0.97±0.05 |
| | | 164 | 2.31±0.11 | 2.39±0.08 | 0.97±0.05 |
| | | 204 | 2.21±0.11 | 2.39±0.08 | 0.93±0.06 |
| | | 305 | 2.31±0.08 | 2.41±0.08 | 0.96±0.05 |
| | | 507 | 2.28±0.12 | 2.43±0.08 | 0.94±0.06 |
| 15604-M2.2 | 38357 | 11 | 1.46±0.05 | 2.38±0.08 | 0.62±0.03 |
| | | 21 | 1.58±0.06 | 2.38±0.08 | 0.66±0.03 |
| | | 41 | 1.58±0.05 | 2.38±0.08 | 0.67±0.03 |
| | | 71 | 1.63±0.07 | 2.38±0.08 | 0.69±0.04 |
| | | 103 | 1.99±0.06 | 2.38±0.08 | 0.83±0.04 |
| | | 133 | 2.16±0.08 | 2.39±0.08 | 0.90±0.05 |
| | | 163 | 2.42±0.08 | 2.39±0.08 | 1.01±0.05 |
| | | 204 | 2.33±0.08 | 2.39±0.08 | 0.97±0.04 |
| | | 304 | 2.35±0.11 | 2.41±0.08 | 0.98±0.06 |
| | | 506 | 2.66±0.09 | 2.43±0.08 | 1.10±0.05 |
| 15613-M3.6 | 38360 | 21 | 1.71±0.06 | 2.38±0.08 | 0.72±0.04 |
| | | 41 | 1.93±0.07 | 2.39±0.08 | 0.81±0.04 |
| | | 61 | 2.08±0.13 | 2.39±0.08 | 0.87±0.06 |
| | | 82 | 2.00±0.07 | 2.39±0.08 | 0.84±0.04 |
| | | 102 | 2.18±0.07 | 2.40±0.08 | 0.91±0.04 |
| | | 127 | 2.02±0.07 | 2.40±0.08 | 0.84±0.04 |
| | | 153 | 2.22±0.09 | 2.40±0.08 | 0.93±0.05 |
| | | 202 | 2.27±0.10 | 2.40±0.08 | 0.95±0.05 |
| | | 304 | 2.25±0.16 | 2.41±0.08 | 0.94±0.07 |
| | | 506 | 2.44±0.09 | 2.42±0.08 | 1.00±0.05 |
| 15620-M3.7 | 38361 | 13 | 1.55±0.05 | 2.38±0.08 | 0.65±0.03 |
| | | 23 | 1.77±0.06 | 2.38±0.08 | 0.74±0.04 |
| | | 42 | 1.90±0.06 | 2.39±0.08 | 0.80±0.04 |
| | | 63 | 1.92±0.06 | 2.39±0.08 | 0.80±0.04 |
| | | 83 | 2.17±0.10 | 2.39±0.08 | 0.91±0.05 |
| | | 103 | 2.04±0.10 | 2.40±0.08 | 0.85±0.05 |
| | | 128 | 1.95±0.10 | 2.40±0.08 | 0.81±0.05 |
| | | 154 | 2.31±0.07 | 2.40±0.08 | 0.96±0.04 |
| | | 255 | 2.35±0.11 | 2.41±0.08 | 0.98±0.06 |
| | | 507 | 2.52±0.09 | 2.42±0.08 | 1.04±0.05 |
| 15627-M3.8 | 38363 | 12 | 1.48±0.06 | 2.38±0.08 | 0.62±0.03 |
| | | 22 | 1.72±0.16 | 2.38±0.08 | 0.72±0.07 |
| | | 33 | 1.77±0.14 | 2.38±0.08 | 0.74±0.07 |
| | | 52 | 1.67±0.05 | 2.39±0.08 | 0.70±0.03 |
| | | 82 | 2.15±0.07 | 2.39±0.08 | 0.90±0.04 |
| | | 104 | 2.04±0.08 | 2.39±0.08 | 0.85±0.04 |
| | | 153 | 2.25±0.12 | 2.40±0.08 | 0.94±0.06 |
| | | 204 | 2.23±0.15 | 2.40±0.08 | 0.93±0.07 |
| | | 304 | 2.32±0.12 | 2.41±0.08 | 0.96±0.06 |
| | | 506 | 2.42±0.10 | 2.42±0.08 | 1.00±0.05 |
| 15632 | 38000 | 1012 | 2.45±0.12 | 2.45±0.08 | 1.00±0.06 |
| | | 1011 | 2.40±0.09 | 2.45±0.08 | 0.98±0.05 |
| | | 1011 | 2.38±0.08 | 2.45±0.08 | 0.97±0.05 |
| | | 1012 | 2.61±0.18 | 2.45±0.08 | 1.07±0.08 |

Table 1 (*continued*)

| Station name and number | Date (dd/mm/yy) | Depth (m) | Total $^{234}$Th (dpm l$^{-1}$) | $^{238}$U (dpm l$^{-1}$) | $^{234}$Th:$^{238}$U |
|---|---|---|---|---|---|
| | | 1012 | 2.44±0.11 | 2.45±0.08 | 1.00±0.06 |
| | | 1012 | 2.42±0.08 | 2.45±0.08 | 0.99±0.05 |
| | | 1012 | 2.46±0.20 | 2.45±0.08 | 1.00±0.09 |
| | | 1012 | 2.39±0.08 | 2.45±0.08 | 0.97±0.04 |
| | | 1012 | 2.55±0.09 | 2.45±0.08 | 1.04±0.05 |

indicates particle export from this parcel (Bacon and Anderson, 1982; Kaufman et al., 1981; Santschi et al., 1979; Tsunogai et al., 1986). A $^{234}$Th:$^{238}$U ratio of $>1$ indicates particle accumulation and perhaps remineralisation (Waples et al., 2006), and a ratio of 1 indicates a situation where $^{234}$Th ingrowth from $^{238}$U is balanced by $^{234}$Th removal and decay. In general the $^{234}$Th:$^{238}$U activity ratios in surface waters were $<1$, ranging from 0.39 to 0.86, and reached a ratio of 1 at depths between 100 and 200 m. In a few instances (Stations M1, M3.1, M7, and M9.1), a ratio of $\approx$1.1 was observed immediately below the surface disequilibrium, suggesting that remineralisation was taking place in the mesopelagic zone. It is interesting to note that ratios of $\approx$1.1 also were measured at greater depths at certain locations (Stations M1, M3.1, M3.2, M6.1, M7, M5, and M2.2), but will not be investigated further in this paper. Fig. 3 shows four example profiles to highlight major points of interest. During leg 1 there was a clear difference between the disequilibria observed north and south of the Crozet Islands: large disequilibria of $<1$ were observed to the north and small disequilibria were observed to the south. This trend was not observed during leg 2: large disequilibria were observed throughout the study site.

### 3.3. Carbon-to-thorium (C:Th) ratios

The C:Th ratios are shown in Table 2. Ratios ranged from 5–10 and 6–11 μmol dpm$^{-1}$ on leg 1 and leg 2, respectively. There are no temporal or spatial large-scale pattens of C:Th ratios, suggesting that small-scale variation is controlling the small range of values that were observed. The small variation in the C:Th ratios is the most striking aspect of the data considering the wide range of bloom conditions that were sampled.

The importance of the C:Th ratio is clear when Eq. (6) is expressed graphically as shown in Fig. 1 of Buesseler et al. (2006). For example, given the same $^{234}$Th disequilibrium a doubling of the C:Th ratio will also result in a doubling of the calculated POC export. The measurement of C:Th ratios has recently received much attention in the literature and has been summarised by Buesseler et al. (2006). Given the importance of the C:Th ratio for estimates of POC export, a conclusion that this is driving the estimates of POC flux should be one that is not dismissed lightly. However, during CROZEX the variation of the C:Th ratio on leg 1 is less than the variation observed in the POC flux estimates, varying by factors of 2 and 3, respectively. In addition to this, the highest C:Th ratio was observed at M6.1, one of the sites of lowest POC flux. During leg 2, this distinction was not present but the generally homogenous nature of both the C:Th ratios and POC fluxes suggests that the C:Th ratio is again not the primary driving parameter of levels of POC flux. The C:Th ratios measured on CROZEX generally agree well with other studies of natural systems in the Polar Front (PF) (Table 3).

## 4. Discussion

### 4.1. $^{234}$Th export fluxes

$^{234}$Th/$^{238}$U disequilibria were integrated to a depth where the $^{234}$Th:$^{238}$U ratio reached 1. If a remineralisation peak was evident above this equilibrium depth, such as the one highlighted in Fig. 3B, the integral of this peak was subtracted from the integrated $^{234}$Th deficit. Integrated $^{234}$Th fluxes (dpm m$^{-2}$ d$^{-1}$) calculated using the SS model (Eq. (3)) for each station are shown in Table 2. For leg 1 $^{234}$Th disequilibria fall into two distinct groups: 573–813 dpm m$^{-2}$ d$^{-1}$ ($\bar{x}$ = 709 dpm m$^{-2}$ d$^{-1}$) and 1619–2352 dpm m$^{-2}$ d$^{-1}$ ($\bar{x}$ = 2026 dpm m$^{-2}$ d$^{-1}$). The first group are Stations M2, M6, and M3.2, and the second group are the other seven stations. The $^{234}$Th flux for M3.2

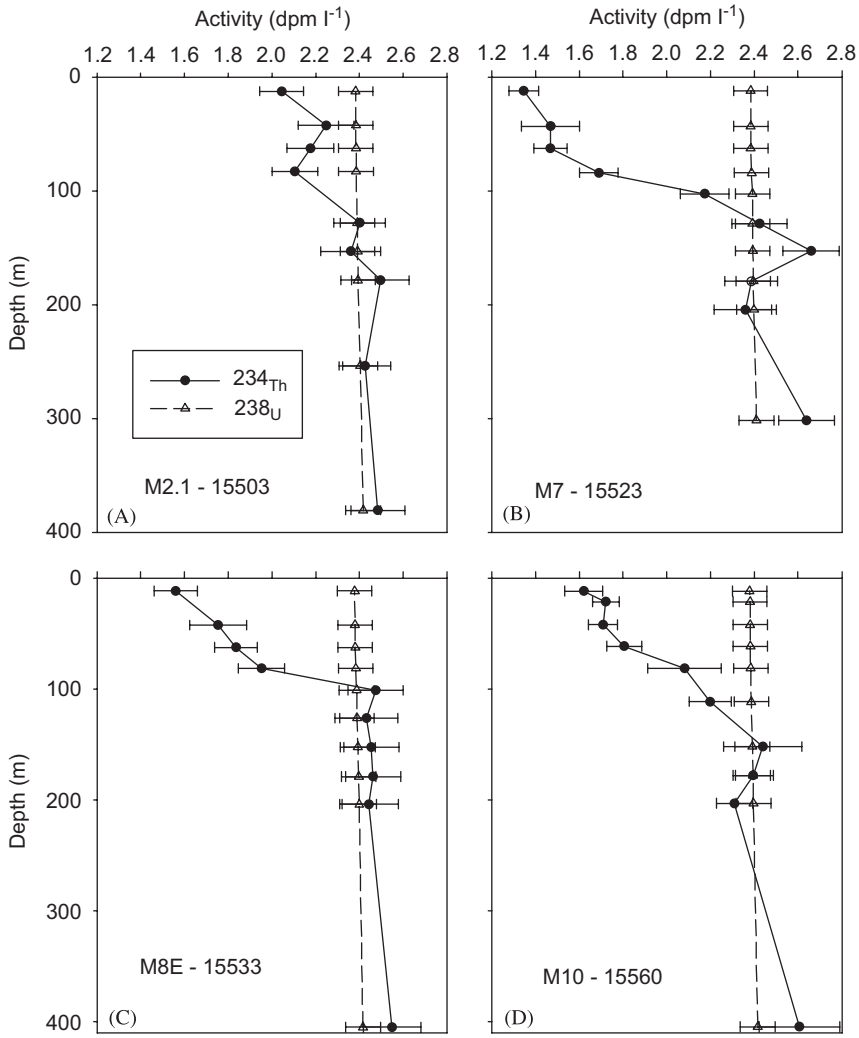


Fig. 3. (A–D) Four example profiles of the $^{234}$Th disequilibria observed. Circles and solid line are total $^{234}$Th activities, and triangles and dashed line are $^{238}$U activities. Error bars are 1$\sigma$ for $^{234}$Th and 3.3% of the calculated $^{238}$U activities. Fig. 3A of Station M2.1 south of the Crozet Islands on leg 1 shows a small $^{234}$Th disequilibrium. A subsurface remineralisation peak is apparent in Fig. 3B at Station M7. At greater depths a $^{234}$Th:$^{238}$U ratio of $>1$ was also evident. Note the $x$-axis starts at 1.2 dpm l$^{-1}$.

appeared to be anomalously low compared to the other leg 1 occupations of M3, but very similar to the fluxes measured for M2 and M6. This was due to advection of water from south of the islands (Pollard et al., 2007b). For leg 2, $^{234}$Th disequilibria do not fall into any distinct groups but formed one group with fluxes ranging from 1744 to 2846 dpm m$^{-2}$ d$^{-1}$ ($\bar{x} = 2306$ dpm m$^{-2}$ d$^{-1}$). The general trend was for higher $^{234}$Th disequilibria during leg 2.

M2, M6, and M9 were each occupied twice during the sampling period with 47, 41, and 16 days, respectively, between subsequent occupations of the same station. Savoye et al. (2006) recommended that the NSS model is most appropriate when reoccupations of the same station are 1–4 weeks apart. This is true for M9 but not for M2 and M6. However, despite the long time interval between the two profiles at M2 and M6, the NSS calculation shown in Eq. (5) was nonetheless applied. In order to apply the NSS model it has to be assumed that the same water mass was sampled on both occasions. To examine this assumption, the salinity profiles were compared between subsequent occupations of the same station. Salinity varied with an average of $0.042 \pm 0.01$, $0.003 \pm 0.004$, and $0.028 \pm 0.03$‰ ($\bar{x} \pm 1\sigma$) for M2, M6, and M9, respectively, between subsequent profiles at the

Table 2
$^{234}$Th (dpm m$^{-2}$ d$^{-1}$), POC (mmol m$^{-2}$ d$^{-1}$) and PON (mmol m$^{-2}$ d$^{-1}$) export fluxes calculated with the steady state model

| Station name and number | Mixed layer depth (m)[a] | Integration depth (m) | $^{234}$Th flux (dpm m$^{-2}$ d$^{-1}$)[b] | C:Th ratio (μmol dpm$^{-1}$) Depth (m)[c] | N:Th ratio (μmol dpm$^{-1}$)[d] | POC export (mmol m$^{-2}$ d$^{-1}$)[b] | PON export (mmol m$^{-2}$ d$^{-1}$)[b] | $^{14}$C primary production (mmol m$^{-2}$ d$^{-1}$)[e] | *ThE* ratio (%)[b] |
|---|---|---|---|---|---|---|---|---|---|
| 15492-M1 | 67 | 158 | 2043±483 (2247±342) | 8.4±0.9 (200) | 1.3±0.1 | 17.1±4.5 (18.8±3.5) | 2.7±0.7 (2.9±0.6) | 90 | 19 (21) |
| 15495-M3.1 | 138 | 182 | 1845±485 (1624±336) | 8.3±0.9 (225) | 1.3±0.1 | 15.3±4.4 (13.5±3.2) | 2.4±0.7 (2.1±0.5) | 44 | 35 (31) |
| 15498-M3.2 | 95 | 103 | 813±380 (821±376) | 6.0±0.7 (200) | 1.1±0.1 | 4.9±2.3 (4.9±2.3) | 0.9±0.4 (0.9±0.4) | 31 | 16 (16) |
| 15503-M2.1 | 113 | 128 | 740±409 (677±361) | 7.2±0.8 (150) | 1.3±0.1 | 5.3±3.0 (4.9±2.7) | 0.9±0.5 (0.9±0.5) | 36 | 15 (14) |
| 15512-M6.1 | 167 | 104 | 573±387 (576±383) | 10.1±1.1 (175) | 1.9±0.2 | 5.8±4.0 (5.8±3.9) | 1.1±0.8 (1.1±0.7) | 20 | 30 (30) |
| 15517-M3.3 | 51 | 156 | 1965±424 (1641±338) | 7.1±0.8 (200) | 1.2±0.1 | 13.9±3.4 (11.6±2.7) | 2.4±0.6 (2.0±0.5) | 40 | 35 (29) |
| 15523-M7 | 79 | 179 | 2352±457 (2467±317) | 5.5±0.7 (150) | 1.1±0.1 | 13.0±3.0 (13.6±2.5) | 2.6±0.6 (2.7±0.5) | 64 | 20 (21) |
| 15533-M8E | 66 | 101 | 1619±349 (1621±347) | 9.4±1.1 (150) | 1.6±0.2 | 15.3±3.8 (15.3±3.8) | 2.5±0.6 (2.6±0.6) | 11 | 133 (133) |
| 15539-M8W | 44 | 103 | 2232±327 (2216±324) | 6.1±0.7 (150) | 0.9±0.1 | 13.7±2.5 (13.6±2.5) | 2.1±0.4 (2.0±0.4) | 41 | 34 (33) |
| 15542-M9.1 | 26 | 122 | 2125±277 (2107±327) | 7.9±0.9 (120) | 1.1±0.1 | 16.8±2.9 (16.7±3.2) | 2.3±0.4 (2.3±0.4) | 57 | 29 (29) |
| 15554-M9.2 | 26 | 175 | 2831±434 (2187±330) | 10.6±1.2 (120) | 1.5±0.2 | 30.0±5.6 (23.2±4.3) | 4.3±0.8 (3.3±0.6) | 10 | 305 (235) |
| 15560-M10 | 43 | 152 | 1744±449 (1603±351) | 7.1±0.8 (110) | 1.3±0.1 | 12.3±3.4 (11.3±2.8) | 2.3±0.6 (2.1±0.5) | 36 | 35 (32) |
| 15574-M3.4 | 77 | 184 | 2524±443 (1957±319) | 10.2±1.1 (180) | 1.7±0.2 | 25.8±5.3 (20.0±3.9) | 4.2±0.9 (3.3±0.6) | 60 | 43 (34) |
| 15580-M5 | 104 | 203 | 2846±485 (2029±333) | 6.3±0.7 (125) | 1.0±0.1 | 17.9±3.6 (12.8±2.5) | 2.9±0.6 (2.1±0.4) | 34 | 52 (37) |
| 15590-M3.5 | 75 | 204 | 2295±503 (1606±346) | 9.7±1.1 (100) | 1.4±0.2 | 22.2±5.4 (15.6±3.8) | 3.2±0.8 (2.2±0.5) | 27 | 81 (57) |
| 15595-M6.2 | 87 | 144 | 2284±382 (1798±326) | 8.0±0.9 (120) | 1.2±0.1 | 18.3±3.6 (14.4±3.0) | 2.8±0.6 (2.2±0.5) | 25 | 73 (57) |
| 15604-M2.2 | 73 | 163 | 2546±397 (2170±310) | 8.7±1.0 (160) | 1.4±0.2 | 22.0±4.2 (18.8±3.4) | 3.5±0.7 (3.0±0.5) | 17 | 128 (109) |
| 15613-M3.6 | 30 | 202 | 1978±466 (1340±325) | 10.3±1.1 (80) | 1.7±0.2 | 20.4±5.3 (13.8±3.7) | 3.3±0.9 (2.2±0.6) | 250 | 8 (6) |
| 15620-M3.7 | 39 | 154 | 1960±416 (1448±335) | 7.0±0.8 (80) | 1.1±0.1 | 13.7±3.3 (10.1±2.6) | 2.2±0.5 (1.7±0.4) | 184 | 7 (5) |
| 15627-M3.8 | 21 | 153 | 2051±416 (1665±340) | 7.3±0.8 (80) | 1.2±0.1 | 15.0±3.5 (12.2±2.8) | 2.5±0.6 (2.1±0.5) | 138 | 11 (9) |

The mixed layer depths (m), integration depths (m) for $^{234}$Th/$^{238}$U disequilibria, and C:Th and N:Th ratios (μmol dpm$^{-1}$) on >50 μm SAPS-filtered particulate matter are given for reference, in addition to primary production (mmol m$^{-2}$ d$^{-1}$) and *ThE* ratios (%). Stations 15492–15542 are leg 1 and 15554–15627 are leg 2.
All errors are 1$\sigma$.

[a]Mixed layer depths were calculated using the method described by Venables et al. (2007).
[b]Values in parenthesis are the fluxes and *ThE* ratios integrated to 100 m for comparison with other studies.
[c]Values in parenthesis are sampling depths for C:Th and N:Th ratios.
[d]N:Th ratios were sampled from the same depth as the C:Th ratios.
[e]Data from Seeyave et al. (2007).

Table 3
C:Th ratios measured in different regions of the Polar Front in the Southern Ocean

| Region/study | Date | Size fraction (μm) | Depth range (m) | C:Th ratio (μmol dpm$^{-1}$) | Reference |
|---|---|---|---|---|---|
| Atlantic | October–November 1992 | >1 | 20–200 | 20.9 (6–12)[a] | Rutgers van der Loeff et al. (1997) |
| Atlantic | December 1995–January 1996 | >1 | >80 | 10.2 | Rutgers van der Loeff et al. (2002) |
| Pacific-AESOPS | October 1997–March 1998 | >70 | 80–150 | 3.0–6.2 | Buesseler et al. (2001) |
| Indian | January–February 1999 | >60 | 100 | 0.8–1.4 | Coppola et al. (2005) |
| Indian-KEOPS | January–February 2005 | 55–210 | 18–129 | 5.9–53.4 | Savoye et al. (2007) |
| Indian-CROZEX | November 2004–February 2005 | >50 | 80–225 | 5.5–10.8 | This study |

[a]POC concentrations were calculate from suspended particulate matter which were then combined with particulate $^{234}$Th data. The ratio of 20.9 μmol dpm$^{-1}$ was then scaled down to 30–60% based on literature data on organic carbon and $^{234}$Th in suspended matter and trap material to give ratios in parenthesis.

Table 4
$^{234}$Th (dpm m$^{-2}$ d$^{-1}$), POC (mmol m$^{-2}$ d$^{-1}$) and PON (mmol m$^{-2}$ d$^{-1}$) export fluxes calculated with a non-steady state model

| Station name | Integration depth (m) | $^{234}$Th flux (dpm m$^{-2}$ d$^{-1}$)[a] | C:Th ratio (μmol dpm$^{-1}$) | N:Th ratio (μmol dpm$^{-1}$) | POC export (mmol m$^{-2}$ d$^{-1}$)[a] | PON export (mmol m$^{-2}$ d$^{-1}$)[a] | *ThE* ratio (%)[a,b] |
|---|---|---|---|---|---|---|---|
| M2 | 120 | 2931±477 (2673±429) | 7.9±0.6 | 1.3±0.1 | 23.3±4.2 (21.2±3.8) | 3.9±0.7 (3.6±0.6) | 88 (80) |
| M6 | 100 | 2326±468 | 9.0±0.7 | 1.6±0.1 | 21.0±4.5 | 3.7±0.8 | 93 |
| M9 | 120 | 2949±956 (2288±823) | 9.3±0.7 | 1.3±0.1 | 27.3±9.1 (21.2±7.8) | 3.8±1.3 (3.0±1.1) | 81 (63) |

The integration depths (m) for $^{234}$Th/$^{238}$U disequilibria and C:Th and N:Th ratios (μmol dpm$^{-1}$) are also given for reference.
All errors are 1$\sigma$.
[a]Values in parenthesis are the fluxes and *ThE* ratios integrated to 100 m for comparison with other studies.
[b]*ThE* ratios were calculated using the average primary production of subsequent occupations of the same station.

same station down to the $^{234}$Th integration depth. M6 showed least variation in salinity and M2 and M9 showed more variation. This is not surprising because M6 is far enough south to be clear of circulation fronts: the sub-Antarctic Front (SAF) and a newly described southern branch of the SAF that skirts to the south of the Crozet Plateau, whereas M9 and M2 are much closer to these circulation fronts (Pollard et al., 2007b). Salinity is one way of assessing whether the same water mass was sampled during subsequent profiles and only reveals if the same type of water is entering the station location. Ideally a surface drifter or conservative tracer such as $SF_6$ would have been released while first sampling a location so that the ship may return to that same parcel of water to sample it again, but the nature of the cruise and project did not allow for such an approach. Consequently, the authors recognise this limitation, and for the purpose of the NSS calculation it was assumed that the same water mass was sampled on subsequent occupations of the same station. In addition to this, term $V$ comprising the advective and turbulent diffusive transport was assumed to be negligible as discussed in Section 2.4. Integrated $^{234}$Th fluxes calculated using the NSS model (Eq. (5)) are shown in Table 4. The fluxes are high both to the north and to the south of the region with $^{234}$Th fluxes ranging from 2326 to 2949 dpm m$^{-2}$ d$^{-1}$. The NSS fluxes compare well with the leg 2 SS fluxes.

Station M3 was visited eight times over the course of two cruises, therefore providing a series of opportunities to take repeated profiles of $^{234}$Th to be used in a NSS analysis. As previously described, in order for a NSS analysis to be applied, the same parcel of water should be sampled; otherwise the analysis runs into complications due to the advective and turbulent diffusive term $V$, which is assumed to be zero in Eqs. (3) and (5). During

various occupations of M3 it was clear that the same parcel of water was not encountered at M3 based on hydrographical observations. In particular, M3.2 was shown to be characteristic of HNLC water that had been advected from south of the Crozet Plateau (Pollard et al., 2007b). In addition to this the last three occupations of M3 were centred in a blooming eddy close to the M3 location (Allen et al., 2006). It was hypothesised by Allen et al. (2006) that the bloom was fuelled by entraining nutrient-rich coastal waters from the local Île de la Possession, which were then vertically mixed with water in the centre of the eddy. Although the general residence time for water entering the bloom area to the north of the islands is typically 62 days (Pollard et al., 2007b) the area immediately north of the islands (M3) is probably experiencing more hydrodynamic variability, thus complicating the use of a NSS model at this site. For the interpretation of M3 fluxes, it needs to be kept in mind that there is an unknown uncertainty resulting from the probable impact of lateral advection and/or a non-steady state. Therefore, only the SS model was applied to the data from M3 due to the uncertainties and highly complex nature of the circulation seen there.

### 4.2. POC and PON export fluxes

The primary, biogeochemical idea to be tested in this paper was whether enhanced POC export was observed in a topographically iron-fertilised bloom (Planquette et al., 2007) in an HNLC region, when compared with control sites. By using calculated $^{234}$Th fluxes, it is possible to estimate the POC flux by multiplying it by the C:Th ratio (Eq. (6); Table 2). POC fluxes for leg 1 fall into the same two distinct groups as those described for the $^{234}$Th disequilibria with Stations M2, M6, and M3.2 showing low POC fluxes (*ca.* 5 mmol C m$^{-2}$ d$^{-1}$) and with high POC fluxes (*ca.* 15 mmol C m$^{-2}$ d$^{-1}$) across the rest of the study site. Leg 2 showed high POC fluxes across the whole region ranging from 12 to 30 mmol C m$^{-2}$ d$^{-1}$. The same procedure is used for calculating PON fluxes using $^{234}$Th fluxes and PON to $^{234}$Th ratios (N:Th). PON fluxes follow the same pattern as POC fluxes: for leg 1 M2, M6, and M3.2 had low PON fluxes (*ca.* 1.0 mmol N m$^{-2}$ d$^{-1}$) whereas high PON fluxes (*ca.* 2.4 mmol N m$^{-2}$ d$^{-1}$) were encountered across the rest of the study site. Leg 2 showed high PON fluxes across the whole region ranging from 2.2 to 4.3 mmol N m$^{-2}$ d$^{-1}$.

To calculate the NSS POC and PON fluxes (Table 4), the $^{234}$Th fluxes were multiplied by the mean of the two C:Th (and N:Th) ratios measured at subsequent occupations of the same station. Generally the NSS fluxes are comparable to the SS fluxes measured during leg 2. In the north at M9 the NSS POC flux of 27.3 mmol C m$^{-2}$ d$^{-1}$ agrees best with the leg 2 SS POC flux of 30.0 mmol C m$^{-2}$ d$^{-1}$. To the south at M2 and M6 the NSS POC fluxes of $\approx$22 mmol C m$^{-2}$ d$^{-1}$ agree well with the leg 2 SS fluxes of $\approx$20 mmol C m$^{-2}$ d$^{-1}$ but are about 4 times higher than the leg 1 SS fluxes. The confirmation of high POC fluxes in the southern region during leg 2 suggest that the small bloom observed there resulted in a reasonable export event. Again, NSS PON fluxes followed the same pattern as the SS PON fluxes. NSS fluxes ranged from 3.7 to 3.9 mmol N m$^{-2}$ d$^{-1}$.

### 4.3. Export efficiency

To put some perspective on the proportion of primary production that is exported out of the surface ocean the *ThE* ratio can be calculated (Buesseler, 1998). The *ThE* ratio is the ratio of $^{234}$Th-derived POC flux to $^{14}$C primary production and is therefore similar in concept to the *f*-ratio which is the ratio of new production to total production (Eppley and Peterson, 1979). Table 2 shows the *ThE* ratios and associated $^{14}$C fixation (mmol m$^{-2}$ d$^{-1}$) measured at each station by Seeyave et al. (2007). Fig. 4 shows how $^{234}$Th-derived POC export varies with $^{14}$C primary production. In general *ThE* ratios are lower during leg 1 than leg 2. Leg 1 *ThE* ratios range from 15% to 35% with the exception of M8E which peaks at 133%. Leg 2 shows much higher variability in *ThE* ratios with low values in the M3 eddy bloom of 7–11%, high values of 35–81% and two values in excess of 100%. *ThE* ratios during CROZEX were almost alway $>$10% which is typical of the Southern Ocean (Buesseler, 1998). Higher *ThE* ratios of 12–24% have been reported by Rutgers van der Loeff et al. (1997) in a Polar Frontal bloom, and Buesseler et al. (2003) reported a wide range of *ThE* ratios from 15% to 65% during a project to assess the effect of an ice margin on production and particle export. Therefore the majority of CROZEX *ThE* ratios agree with values reported in the literature. *ThE* ratios calculated from the NSS POC fluxes at M2, M6, and M9 were 98%, 93%, and 81%, respectively (Table 4).

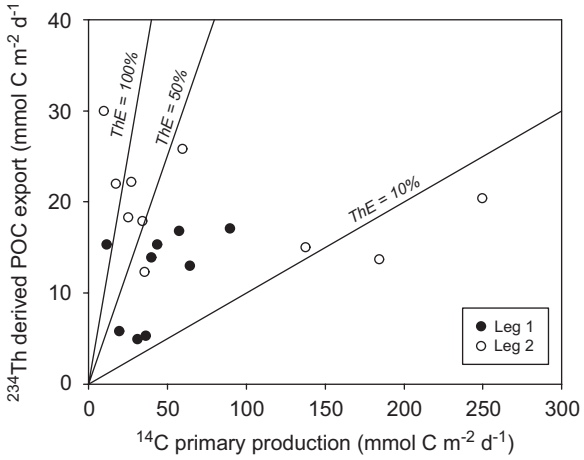


Fig. 4. *ThE* ratios for stations sampled for $^{234}$Th-derived POC export (mmol C m$^{-2}$ d$^{-1}$) and $^{14}$C-derived primary production (mmol C m$^{-2}$ d$^{-1}$), the latter measured by Seeyave et al. (2007). For reference the 10%, 50%, and 100% *ThE* ratio lines have been plotted.

Although the *ThE* ratio can be used to assess the POC export efficiency of a bloom, some caution should be exercised when interpreting the results. In particular, the two properties used to generate the *ThE* parameter operate on different time-scales. $^{14}$C primary production is a rate measurement typically measured with 12–24 h bottle incubations whereas $^{234}$Th export estimates integrate over the mean lifetime of the tracer, which is 34.8 days (Buesseler, 1998). Given this large difference in time-scales it is easy to see how one might arrive at a *ThE* ratio of $>100\%$. For example, should a $^{14}$C measurement be made on a particularly cloudy day the measured rates of primary production are likely to be depressed and the consequent *ThE* ratio enhanced. This could result in two different conclusions as to the export efficiency of the bloom: a low *ThE* ratio in the case of the sunny day (with high primary production) or a high *ThE* ratio in the case of the cloudy day (with low primary production). This issue is of relevance in an area of dynamic meteorological activity, such as the Southern Ocean, and worthy of future investigation. In addition to the scenario just described, a variety of other factors can contribute to difficulties in interpreting *ThE* ratios such as the onset or decline of a bloom or a particularly efficient biological pump (Buesseler, 1998).

Given the many factors that are involved in potentially driving the *ThE* ratio of the Crozet bloom, the *ThE* ratios calculated in Table 2 have to be treated with some caution. However, keeping this caveat in mind, some conclusions can be drawn from the CROZEX *ThE* ratios, in particular, the general trend to higher *ThE* ratios observed during leg 2. The most likely cause of these are the decline and termination of the bloom resulting in an instantaneously efficient biological pump. However, a stable bloom supporting a continuously efficient biological pump can not be ruled out except in the cases of where *ThE* ratios exceed 100%, which clearly have to result from an offset of the characteristic time-scales of the measured parameters.

### 4.4. Comparison with other Southern Ocean $^{234}$Th studies

Since SOIREE, the first iron fertilisation experiment in the Southern Ocean in February 1999, there have been three other such experiments: EisenEx in November 2000, SOFeX in January–February 2002, and EIFEX in January–March 2004 (Boyd et al., 2000; Gervais et al., 2002; Coale et al., 2004; Hoffmann et al., 2006). All these experiments followed the same general pattern whereby an area of the ocean was artificially fertilised with iron and then the ensuing biological response was monitored in the patch of fertilisation, with a control site outside of the iron fertilised area. All these experiments noted an increase in biomass in the patch of fertilisation, but have yielded varying results in the amount of POC flux to mesopelagic depths when compared to their respective control sites and/or to observations made in the same oceanic region during a different time period. The SOIREE and EisenEx blooms, which were monitored for 13 and 22 days, respectively, showed no significant enhancement of POC export in the iron fertilised area (Nodder et al., 2001; Charette and Buesseler, 2000; Rutgers van der Loeff and Vöge, 2001). However, the SOFeX bloom that was monitored for 27 days, showed 2.5 times more POC flux within the iron-fertilised patch when compared to outside the patch (Buesseler et al., 2004, 2005). Although the SOFeX POC flux measured was still smaller than a natural bloom at the same site in 1998 (Buesseler et al., 2001). EIFEX, which was monitored for 36 days, recorded the highest POC flux ever measured in the Southern Ocean in addition to generally higher POC fluxes within the iron-fertilised patch (Vöge et al., 2006).

After SOFeX, Bishop et al. (2004) concluded that POC export only showed a significant increase several weeks after the first iron addition, with fluxes peaking at day 41. Unfortunately these experiments are usually restricted in time, therefore allowing the ship to be present in the study site for the release of iron and initial bloom development but not for the bloom termination when particle export is likely to be highest (Buesseler and Boyd, 2003; Buesseler et al., 2005). This may explain why the shorter iron-fertilisation experiments showed less POC export than the longer experiments.

CROZEX did not suffer from the issue of restricted time because the bloom area was fertilised naturally with iron from the Crozet Plateau (Charette et al., 2007; Planquette et al., 2007), thus allowing the study to focus its sampling on the later half of the bloom period. The first observation of $^{234}$Th-derived POC flux on CROZEX was made about 15 days after the chlorophyll peak of the main bloom in the north of the study site (Venables et al., 2007) with observations then made across the study site for 2 months, hence during the decline of the bloom. This time frame should give the opportunity to resolve the lack of data from the declining phase of a phytoplankton bloom, but before this is done the CROZEX $^{234}$Th-derived POC fluxes should be compared to other $^{234}$Th POC fluxes made in the Southern Ocean under natural conditions.

There have been several studies into $^{234}$Th-derived POC fluxes in the PFZ in the Southern Ocean (Rutgers van der Loeff et al., 1997, 2002; Buesseler et al., 2001; Coppola et al., 2005). Within the PFZ of the Indian sector of the Southern Ocean, the area in which the Crozet Plateau lies (Pollard et al., 2002), Coppola et al. (2005) obtained $^{234}$Th-derived POC flux estimates in January-February 1999 on the ANTARES 4 cruise, approximately 10°E of the Crozet Islands in an area known as the Crozet Basin. This area is northwest of the Kerguelen Plateau in a deep basin ($\approx$5000 m depth) and away from any significant bottom topography. During this study, very low fluxes of POC were measured, ranging from 0.1 to $-2.5$ mmol C m$^{-2}$ d$^{-1}$ at 100 m, which are less than half the lowest fluxes measured to the south of the CROZEX study site through the same depth horizon (Table 2). Coppola et al. (2005) hypothesised that these resulted from either a very efficient remineralisation process and/or a high bacterial activity, or a decoupling of primary production and POC export. The low abundance of diatoms, which are typical of Southern Ocean Polar Frontal blooms, was also hypothesised to contribute to the low fluxes. In other regions of the Southern Ocean, POC fluxes at 100 m in the PF were estimated to be 19.5–39.1 and 8.8 mmol C m$^{-2}$ d$^{-1}$ (Atlantic PF blooms Rutgers van der Loeff et al., 1997, 2002), and 5.5–14.5 mmol C m$^{-2}$ d$^{-1}$ (Pacific PF blooms Buesseler et al., 2001). The CROZEX data fit well within the range of these Polar Frontal observations.

The most relevant study for comparison with the CROZEX project is the KErguelen Ocean and Plateau compared Study (KEOPS), which sampled the annual bloom observed over the Kerguelen Plateau during January–February 2005 (Blain et al., 2007), and partly overlapped CROZEX. $^{234}$Th POC fluxes measured within the Fe-replete bloom reference station on KEOPS gave POC fluxes at 100 m of 10.5–38.4 mmol C m$^{-2}$ d$^{-1}$ (Savoye et al., 2007), which is generally in good agreement with bloom fluxes measured at 100 m, ranging from 10.1 to 23.2 mmol C m$^{-2}$ d$^{-1}$ on CROZEX (Table 2), if slightly greater in range. This compares to a 100 m POC flux of 12.2 mmol C m$^{-2}$ d$^{-1}$ in the control, non-bloom reference station on KEOPS, which is greater than the 100 m flux observed on CROZEX during leg 1 of 5 mmol C m$^{-2}$ d$^{-1}$, but less than the flux of 14.4–18.8 mmol C m$^{-2}$ d$^{-1}$ during leg 2. However, the average 100 m POC flux of all the CROZEX non-bloom stations was 10 mmol C m$^{-2}$ d$^{-1}$ (Table 2), in very close agreement with KEOPS. The ratio during KEOPS showed a trend of increasing export efficiency at the low productivity site when compared to the high-productivity sites. 58% of primary production was exported below 100 m at the non-bloom reference station, compared with 13–48% being exported below 100 m at the Fe-replete bloom station. A similar, but less clear-cut trend was evident during CROZEX. For CROZEX on leg 1 the export efficiency at 100 m was 16–30% and 21–133% for non-bloom and bloom stations, respectively (Table 2). If the value of 133% for bloom stations is removed, as this is clearly due to a decoupling of primary production and export production, then the range narrows to 21–33% and is almost the same as the non-bloom observations and in close agreement with the KEOPS range of 13–48%. However, on leg 2 after a small bloom had occurred in the south on CROZEX (Venables et al., 2007), the export efficiency at 100 m had changed to 57–109%, 32–235%, and 5–9% for non-bloom, bloom and M3 eddy bloom stations, respectively (Table 2). Once again if

the *ThE* ratios of >100% are removed, the export efficiencies change to 57%, 32–57%, and 5–9% for non-bloom, bloom and M3 eddy bloom stations respectively. Therefore, a trend of decreasing *ThE* ratio with increasing productivity can be seen. These results not only support the KEOPS results but are also in agreement with resent work published by Lam and Bishop (2007) on high-biomass low-export regimes in the Southern Ocean.

### 4.5. Comparison with CROZEX primary and new production estimates

The CROZEX project benefits from its multi-disciplinary nature and wide range of parameters measured. In addition to the $^{234}$Th approach several other methods were used during the CROZEX cruise to estimate new and export production. These were neutrally buoyant sediment traps (Salter et al., 2007), $^{15}$N uptake rates (Lucas et al., 2007), and nutrient-drawdown budgets (Sanders et al., 2007). Each of these is an alternative method of constraining export estimates, assuming that new and export production are equivalent when integrated over at least one annual cycle (Eppley and Peterson, 1979). To clarify terminology for this section: primary production will refer to total carbon assimilation, new production (which relates to the export from the euphotic zone of both particulate and dissolved material (Bronk et al., 1994)) will refer to production resulting from sources of nutrients from outside the euphotic zone, and export production will refer to POC that has settled out of the surface ocean.

Of the other methods used to constrain export during CROZEX the nutrient-drawdown budgets of Sanders et al. (2007) provide the best comparison with the $^{234}$Th-derived POC fluxes. This is because the nutrient-drawdown approach operates on a similar time-scale as the $^{234}$Th approach. Sanders et al. (2007) calculated levels of temporally integrated primary and new production. Temporally integrated primary production was calculated by coupling the chlorophyll to production relationship derived by Seeyave et al. (2007) and satellite chlorophyll imagery. Temporally integrated new production was calculated by determining nitrate removal. Both these parameters, primary and new production, show a clear north–south gradient with high levels in the north and low levels in the south (Fig. 5A and B).

Estimates of $^{234}$Th-derived POC export from the study region during leg 1 show a clear north–south

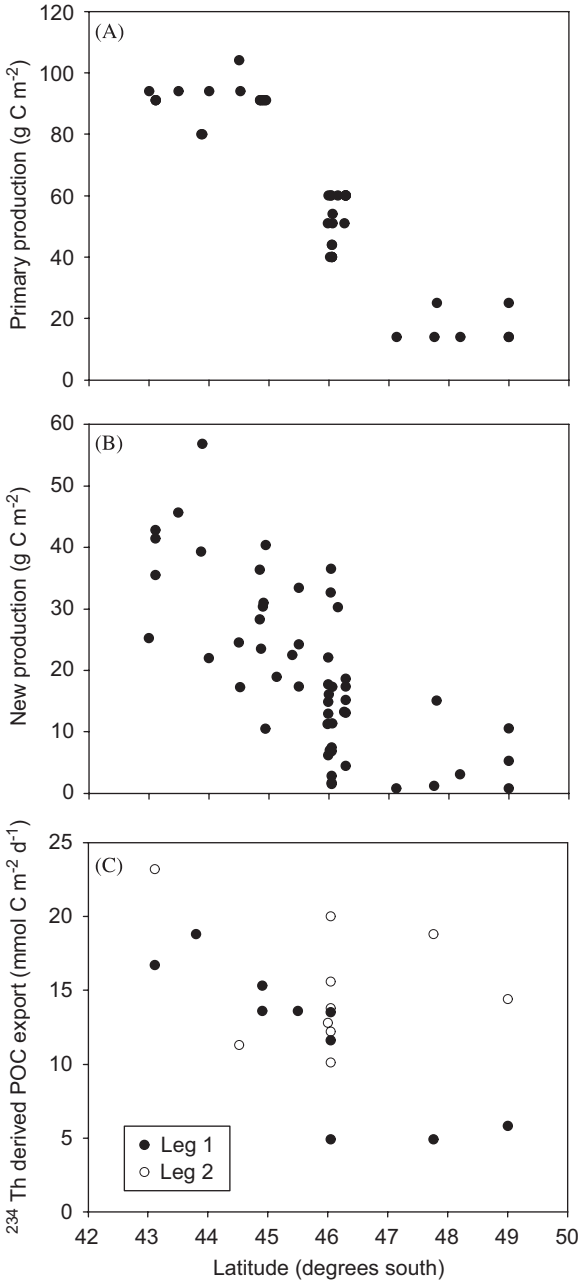


Fig. 5. The latitudinal variation in total primary production (A), new production (B), and $^{234}$Th-derived POC export (C). Satellite-derived primary production and new production are integrated from the start of the bloom period until the date of sampling (Sanders et al., 2007). Not all the units on the *y*-axis are the same: primary and new production are displayed in g C m$^{-2}$ (integrating over the sampling period) and export production is displayed in mmol C m$^{-2}$ d$^{-1}$ thus not allowing a direct comparison. Although there is a time-scale difference between the POC flux and both primary and new production, this should be somewhat dampened by the integrating properties of the $^{234}$Th method which quasi-integrates over the mean lifetime of the tracer (34.8 days).

gradient with values of $\approx 15\,mmol\,C\,m^{-2}\,d^{-1}$ in the north during the period immediately following the phytoplankton bloom, and $\approx 5\,mmol\,C\,m^{-2}\,d^{-1}$ in the south prior to the small southern plankton bloom (Fig. 5C). During leg 2 no gradient was seen once the modest bloom had occurred in the south but ranged by approximately a factor of two across the study region from about 10 to $23\,mmol\,C\,m^{-2}\,d^{-1}$. Both SS and NSS analyses of the $^{234}$Th data suggest no significant north–south gradient of $^{234}$Th-derived POC export existed during this leg, thus the results presented here do not support a higher level of POC export in the large bloom to the north when compared to the small bloom in the south (Fig. 5C).

Sanders et al. (2007) and Seeyave et al. (2007) concluded that primary and new production varied by approximately a factor of 4 between the most northen and southern sites (Fig. 5A and B). While, during leg 1 $^{234}$Th-derived export also showed a north–south gradient, it failed to show the same clear north–south gradient during leg 2 (Fig. 5C). It is worth mentioning at this point that not all the units used in Fig. 5 are the same. Primary and new production are displayed in $g\,C\,m^{-2}$ and export production is displayed in $mmol\,C\,m^{-2}\,d^{-1}$, thus not allowing a direct comparison. However, this does not invalidate the comparison of the north–south trends observed, which have three possible explanations:

(1) the bulk export event from the northern bloom may not have been sampled due to arrival in the region 2 weeks after the peak of the bloom,
(2) the estimates of new production and/or export production are inaccurate, or
(3) new and export production are not equivalent, with this lack of equivalence being particularly pronounced in the north.

These three possibilities will now be examined.

**Explanation 1.** The bulk export event from the northern bloom may not have been sampled due to arrival in the region 2 weeks after the peak of the bloom.

$^{234}$Th-derived POC fluxes are representative of the flux condition over the mean lifetime of the tracer, that is 34.8 days (Buesseler, 1998). Therefore $^{234}$Th-derived fluxes have a natural temporal integrating power built into the tracer. The CROZEX cruise arrived in the study region 2 weeks after the peak of the bloom, which is a shorter time period than the half-life of $^{234}$Th, thus weakening the strength of this explanation.

**Explanation 2.** The estimates of new production and/or export production are inaccurate.

The possibility that the methods used are generating inaccurate results is an issue that frequently arrises and likewise neither the nutrient drawdown nor the $^{234}$Th method are free of flaws or caveats. For example, issues may have arisen in the new production estimates resulting from mesoscale spatial variability in nitrate concentrations (Sanders et al., 2007), or with the $^{234}$Th method when incorporating uncertainties such as the C:Th ratio and the issues related to advection and turbulent diffusion. Given that these issues have been addressed already with the caveats already spoken to, another explanation and hypothesis will be proposed to explain the observed trends and discrepancies seen in the new and export production estimates, based on the assumption that the new and export production estimates are correct.

**Explanation 3.** New and export production are not equivalent, with this lack of equivalence being particularly pronounced in the north.

The paradox to be tackled is why do the patterns of new and export production not agree? When new production takes place it generates organic carbon, essentially the organic carbon that makes up the primary producers: POC and PON. This organic matter then has several possible fates: (1) it ''dies'' and sinks out, (2) it enters a buoyant or very slowly settling organic particulate phase, (3) it enters the dissolved organic pool, (4) it is grazed and moves to a higher trophic level-which will ultimately enter routes 1, 2, or 3 nonetheless. The first pathway is the exported production and can be regarded as the particle flux measured with the $^{234}$Th technique, with a 100 m flux of approximately $12–23\,mmol\,C\,m^{-2}\,d^{-1}$ and $2.0–3.3\,mmol\,N\,m^{-2}\,d^{-1}$ (Table 2). Evidence for the second pathway playing a role has been observed by Sanders et al. (unpublished data) with a POC build up in the surface waters of approximately $12–18\,\mu mol\,C\,l^{-1}$ and $1.8–2.8\,\mu mol\,N\,l^{-1}$ over the course of the sampling period.

Some evidence for the third pathway has been seen in the concentration of the dissolved organic nitrogen (DON) pool over the course of the cruise. A subset of DON samples has been measured

according to Sanders and Jickells (2000) and has shown that on first arrival in the northern part of the study region the surface DON was approximately 5.3 $\mu mol\,N\,l^{-1}$, which then declined to approximately 3.2 $\mu mol\,N\,l^{-1}$ at the end of the sampling period. In contrast to this, the southern region showed a relatively constant level of DON throughout the sampling period of approximately 2.7 and 2.5 $\mu mol\,N\,l^{-1}$ at the start and end of the sampling period respectively (Morris et al., unpublished data). A build up of DON during the first phase of the bloom (which could not be sampled) followed by a decrease of DON (as detected) is not an unreasonable suggestion, as this type of organic matter storage has been observed in another high-latitude setting, the Irminger Basin (Sanders et al., 2005). The elevated levels of DON to the north on first arrival may therefore have been even higher prior to arrival given that the peak of the bloom to the north occurred approximately two weeks before sampling commenced (Venables et al., 2007). This is interesting because the moderate bloom to the south occurred during the sampling period and as yet no evidence of a DON buildup in this region has become apparent. This then opens the question of differential export efficiencies in these two different settings with potentially a high-biomass low-export regime in the productive north and a low-biomass high-export regime in the south (Lam and Bishop, 2007). Therefore, in the context of the Crozet region it is proposed that the high-production region is characterised with low fractional levels of export, in contrast to the low-production region which is characterised with high fractional levels of export.

## 5. Conclusions

It has been demonstrated here that POC export during the Crozet bloom showed high levels in the bloom area and low levels at the southern control stations during leg 1. After a moderately small bloom at the southern control stations this spatial variability was not observed during leg 2, which showed equally high levels of POC export throughout the study site. Therefore, maybe the question that should be asked is not: "Why are the POC fluxes so high at the southern control stations during leg 2?", but instead: "Why are the POC fluxes not even higher at the northern bloom stations?" It is hypothesised that this lack of latitudinal variability in POC export flux was due to a buildup of buoyant particulate and dissolved phases in the northern bloom region, with this hypothesis strengthened by the existence of higher DON concentrations within the northern bloom region. This may then have the effect of reducing the amount of POC that is available for export to mesopelagic depths.

## Acknowledgements

The work that went towards this report would not have been possible without the support and assistance of many people. Thanks goes out to the captain and crew of the R.R.S. *Discovery* on D285 and D286. Thanks to Bob Head for processing POC/N samples at Plymouth Marine Laboratory. This manuscript was greatly improved with very constructive reviews from Nicolas Savoye and one anonymous reviewer, and with comments on an early draft from Richard Lampitt. I wish to thank all the CROZEX scientists for numerous discussions and chats about export and everything else that goes with it, in particular Hugh Venables and Alberto Naveira Garabato for help on the physics. Last but not least a big thank you to Raymond Pollard and Richard Sanders, the true driving force behind CROZEX. Funding for CROZEX came from the NERC core strategic programme, BICEP. Studentship funding (to P.J.M.) was jointly supplied by the School of Ocean and Earth Science, University of Southampton and NERC's old George Deacon Division.

## References

Allen, J., Bakker, D., Read, J., Pollard, R., Charette, M., Venables, H., Planquette, H., Morris, P., Sanders, R., Moore, C.M., Seeyave, S., 2006. An 'eddy-centric' bloom north of the Crozet Islands; sub-mesoscale entrainment of island nutrients or vertical diffusion? In: Challenger Conference for Marine Science, Oban, Scotland.

Bacon, M.P., Anderson, R.F., 1982. Distribution of thorium isotopes between dissolved and particulate forms in the deep sea. Journal of Geophysical Research 87, 2045–2056.

Bacon, M.P., Rutgers van der Loeff, M.M., 1989. Removal of thorium-234 by scavenging in the bottom nepheloid layer of the ocean. Earth and Planetary Science Letters 92, 157–164.

Bacon, M.P., Cochran, J.K., Hirschberg, D., Hammer, T.R., Fleer, A.P., 1996. Export flux of carbon at the equator during the EqPac time-series cruises estimated from $^{234}Th$ measurements. Deep-Sea Research II 43, 1133–1154.

Bhat, S.G., Krishnaswami, S., Lal Rama, D., Moore, W.S., 1969. $^{234}Th/^{238}U$ ratios in the ocean. Earth and Planetary Science Letters 5, 483–491.

Bishop, J.K.B., Edmond, J.M., Ketten, D.R., Bacon, M.B., Silker, W.B., 1977. The chemistry, biology and vertical flux of particulate matter from the upper 400 m of the equatorial Atlantic Ocean. Deep-Sea Research I 24, 511–548.

Bishop, J.K.B., Wood, T.J., Davis, R.E., Sherman, J.T., 2004. Robotic observations of enhanced carbon biomass and export at 55°S during SOFeX. Science 304, 417–420.

Blain, S., Treguer, P., Belviso, S., Bucciarelli, E., Denis, M., Desabre, S., Fiala, M., Jezequel, V.M., Le Fevre, J., Mayzaud, P., Marty, J.C., Razouls, S., 2001. A biogeochemical study of the island mass effect in the context of the iron hypothesis: Kerguelen Islands, Southern Ocean. Deep-Sea Research I 48, 163–187.

Blain, S., Quéguiner, B., Armand, L., Belviso, S., Bombled, B., Bopp, L., Bowie, A., Brunet, C., Brussaard, C., Carlotti, F., Christaki, U., Corbière, A., Durand, I., Ebersbach, F., Fuda, J.-L., Garcia, N., Gerringa, L., Griffiths, B., Guigue, C., Guillerm, C., Jacquet, S., Jeandel, C., Laan, P., Lefèvre, D., Lo Monaco, C., Malits, A., Mosseri, J., Obernosterer, I., Park, Y.-H., Picheral, M., Pondaven, P., Remenyi, T., Sandroni, V., Sarthou, G., Savoye, N., Scouarnec, L., Souhaut, M., Thuiller, D., Timmermans, K., Trull, T., Uitz, J., van-Beek, P., Veldhuis, M., Vincent, D., Viollier, E., Vong, L., Wagener, T., 2007. Impacts of natural iron fertilisation on carbon sequestration in the Southern Ocean. Nature 446, 1070–1074.

Boyd, P.W., Watson, A.J., Law, C.S., Abraham, E.R., Trull, T., Murdoch, R., Bakker, D.C.E., Bowie, A.R., Buesseler, K.O., Chang, H., Charette, M., Croot, P., Downing, K., Frew, R., Gall, M., Hadfield, M., Hall, J., Harvey, M., Jameson, G., LaRoche, J., Liddicoat, M., Ling, R., Maldonado, M.T., McKay, R.M., Nodder, S., Pickmere, S., Pridmore, R., Rintoul, S., Safi, K., Sutton, P., Strzepek, R., Tanneberger, K., Turner, S., Waite, A., Zeldis, J., 2000. A mesoscale phytoplankton bloom in the polar Southern Ocean stimulated by iron fertilization. Nature 407, 695–702.

Boyd, P.W., Law, C.S., Wong, C.S., Nojiri, Y., Tsuda, A., Levasseur, M., Takeda, S., Rivkin, R., Harrison, P.J., Strzepek, R., Gower, J., McKay, R.M., Abraham, E., Arychuk, M., Barwell-Clarke, J., Crawford, W., Crawford, D., Hale, M., Harada, K., Johnson, K., Kiyosawa, H., Kudo, I., Marchetti, A., Miller, W., Needoba, J., Nishioka, J., Ogawa, H., Page, J., Robert, M., Saito, H., Sastri, A., Sherry, N., Soutar, T., Sutherland, N., Taira, Y., Whitney, F., Wong, S.K.E., Yoshimura, T., 2004. The decline and fate of an iron-induced subarctic phytoplankton bloom. Nature 428, 549–553.

Bronk, D.A., Glibert, P.M., Ward, B.B., 1994. Nitrogen uptake, dissolved organic nitrogen release, and new production. Science 265, 1843–1846.

Bucciarelli, E., Blain, S., Tréguer, P., 2001. Iron and manganese in the wake of the Kerguelen Islands (Southern Ocean). Marine Chemistry 73, 21–36.

Buesseler, K.O., 1998. The decoupling of production and particulate export in the surface ocean. Global Biogeochemical Cycles 12, 297–310.

Buesseler, K.O., Boyd, P.W., 2003. Will ocean fertilization work? Science 300, 67–68.

Buesseler, K.O., Bacon, M.P., Cochran, J.K., Livingston, H.D., 1992. Carbon and nitrogen export during the JGOFS North Atlantic Bloom Experiment from $^{234}$Th:$^{238}$U disequilibrium. Deep-Sea Research I 39, 1115–1137.

Buesseler, K.O., Andrews, J.A., Hartman, M.C., Belastock, R., Chai, F., 1995. Regional estimates of the export flux of particulate organic carbon derived from thorium-234 during the JGOFS EqPac program. Deep-Sea Research II 42, 777–804.

Buesseler, K.O., Ball, L., Andrews, J., Benitez-Nelson, C., Belastock, R., Chai, F., Chao, Y., 1998. Upper ocean export of particulate organic carbon in the Arabian Sea derived from thorium-234. Deep-Sea Research II 45, 2461–2487.

Buesseler, K.O., Ball, L., Andrews, J., Cochran, J.K., Hirschberg, D.J., Bacon, M.P., Fleer, A., Brzezinski, M., 2001. Upper ocean export of particulate organic carbon and biogenic silica in the Southern Ocean along 170°W. Deep-Sea Research II 48, 4275–4297.

Buesseler, K.O., Barber, R.T., Dickson, M.-L., Hiscock, M.R., Moore, J.K., Sambrotto, R., 2003. The effect of marginal ice-edge dynamics on production and export in the Southern Ocean along 170°W. Deep-Sea Research II 50, 579–603.

Buesseler, K.O., Andrews, J.E., Pike, S.M., Charette, M.A., 2004. The effects of iron fertilization on carbon sequestration in the Southern Ocean. Science 304, 414–417.

Buesseler, K.O., Andrews, J.E., Pike, S.M., Charette, M.A., Goldson, L.E., Brzezinski, M.A., Lance, V.P., 2005. Particle export during the Southern Ocean Iron Experiment (SOFeX). Limnology and Oceanography 50, 311–327.

Buesseler, K.O., Benitez-Nelson, C.R., Moran, S.B., Burd, A., Charette, M., Cochran, J.K., Coppola, L., Fisher, N.S., Fowler, S.W., Gardner, W.D., Guo, L.D., Gustafsson, O., Lamborg, C., Masque, P., Miquel, J.C., Passow, U., Santschi, P.H., Savoye, N., Stewart, G., Trull, T., 2006. An assessment of particulate organic carbon to thorium-234 ratios in the ocean and their impact on the application of $^{234}$Th as a POC flux proxy. Marine Chemistry 100, 213–233.

Charette, M.A., Buesseler, K.O., 2000. Does iron fertilization lead to rapid carbon export in the Southern Ocean. Geochemistry, Geophysics, Geosystems 1, this issue.

Charette, M.A., Moran, S.B., 1999. Rates of particle scavenging and particulate organic carbon export estimated using $^{234}$Th as a tracer in the subtropical and equatorial Atlantic Ocean. Deep-Sea Research II 46, 885–906.

Charette, M.A., Gonneea, M.E., Morris, P., Statham, P., Fones, G., Planquette, H., Salter, I., Naveira Garabato, A., 2007. Radium isotopes as tracers of iron sources fueling a Southern Ocean phytoplankton bloom. Deep-Sea Research II, in press, doi:10.1016/j.dsr2.2007.06.003.

Chen, J.H., Edwards, L., Wasserburg, G.J., 1986. $^{238}$U, $^{234}$U and $^{232}$Th in seawater. Earth and Planetary Science Letters 80, 241–251.

Chisholm, S.W., Falkowski, P.G., Cullen, J.J., 2001. Discrediting ocean fertilization. Science 294, 309–310.

Coale, K.H., Bruland, K.W., 1985. $^{234}$Th:$^{238}$U disequilibria within the California Current. Limnology and Oceanography 30, 22–33.

Coale, K.H., Bruland, K.W., 1987. Oceanic stratified euphotic zone as elucidated by $^{234}$Th:$^{238}$U disequilibria. Limnology and Oceanography 32, 189–200.

Coale, K.H., Johnson, K.S., Fitzwater, S.E., Gordon, R.M., Tanner, S., Chavez, F.P., Ferioli, L., Sakamoto, C., Rogers, P., Millero, F., Steinberg, P., Nightingale, P., Cooper, D., Cochlan, W.P., Landry, M.R., Constantinou, J., Rollwagen, G., Trasvina, A., Kudela, R., 1996. A massive phytoplankton bloom induced by an ecosystem-scale iron fertilization

experiment in the equatorial Pacific Ocean. Nature 383, 495–501.

Coale, K.H., Johnson, K.S., Chavez, F.P., Buesseler, K.O., Barber, R.T., Brzezinski, M.A., Cochlan, W.P., Millero, F.J., Falkowski, P.G., Bauer, J.E., Wanninkhof, R.H., Kudela, R.M., Altabet, M.A., Hales, B.E., Takahashi, T., Landry, M.R., Bidigare, R.R., Wang, X.J., Chase, Z., Strutton, P.G., Friederich, G.E., Gorbunov, M.Y., Lance, V.P., Hilting, A.K., Hiscock, M.R., Demarest, M., Hiscock, W.T., Sullivan, K.F., Tanner, S.J., Gordon, R.M., Hunter, C.N., Elrod, V.A., Fitzwater, S.E., Jones, J.L., Tozzi, S., Koblizek, M., Roberts, A.E., Herndon, J., Brewster, J., Ladizinsky, N., Smith, G., Cooper, D., Timothy, D., Brown, S.L., Selph, K.E., Sheridan, C.C., Twining, B.S., Johnson, Z.I., 2004. Southern Ocean iron enrichment experiment: carbon cycling in high- and low-Si waters. Science 304, 408–414.

Cochran, J.K., Barnes, C., Achman, D., Hirschberg, D.J., 1995. Thorium-234/Uranium-238 disequilibrium as an indicator of scavenging rates and partuiculate organic carbon fluxes in the Northeast Water Polynya, Greenland. Journal of Geophysical Research 100, 4399–4410.

Cochran, J.K., Roberts, K.A., Barnes, C., Achman, D., 1997. Radionuclides as indicators of particle and carbon dynamics on the East Greenland Shelf. In: Germain, P., et al. (Eds.), Radioprotection-colloques, 32(C2), Proceedings of RADOC 96–97 'Radionuclides in the Oceans'. Institute de Protection et de Surete nucleaire, Cherbourg, France, pp. 129–136.

Cochran, J.K., Buesseler, K.O., Bacon, M.P., Wang, H.W., Hirschberg, D.J., Ball, L., Andrews, J., Crossin, G., Fleer, A., 2000. Short-lived thorium isotopes ($^{234}$Th, $^{228}$Th) as indicators of POC export and particle cycling in the Ross Sea, Southern Ocean. Deep-Sea Research II 47, 3451–3490.

Coppola, L., Roy-Barman, M., Mulsow, S., Povinec, P., Jeandel, C., 2005. Low particulate organic carbon export in the frontal zone of the Southern Ocean (Indian sector) revealed by $^{234}$Th. Deep-Sea Research I 52, 51–68.

Deacon, G., 1984. The Antarctic Circumpolar Ocean. Cambridge University Press, Cambridge.

Delanghe, D., Bard, E., Hamelin, B., 2002. New TIMS constraints on the uranium-238 and uranium-234 in seawaters from the main ocean basins and the Mediterranean Sea. Marine Chemistry 80, 79–93.

Dunne, J.P., Murray, J.W., 1999. Sensitivity of $^{234}$Th export to physical processes in the central equatorial Pacific. Deep-Sea Research I 46, 831–854.

Ehrhardt, M., Koeve, W., 1999. Determination of particulate organic carbon and nitrogen, chapter 17. In: Grasshoff, K., Kremling, K., Ehrhardt, M. (Eds.), Methods of Seawater Analysis. Wiley–VCH, Weinheim.

Eppley, R.W., Peterson, B.J., 1979. Particulate organic matter flux and planktonic new production in the deep ocean. Nature 282, 677–680.

Fowler, S.W., Knauer, G.A., 1986. Role of large particles in the transport of elements and organic compounds through the oceanic water column. Progress in Oceanography 16, 147–194.

Gervais, F., Riebesell, U., Gorbunov, M.Y., 2002. Changes in primary productivity and chlorophyll *a* in response to iron gertilization in the Southern Polar Frontal Zone. Limnology and Oceanography 47, 1324–1335.

Gustafsson, Ö., Buesseler, K.O., Geyer, W.R., Moran, S.B., Gschwend, P.M., 1998. An assessment of the relative importance of horizontal and vertical transport of the particle-reactive chemicals in the coastal ocean. Continental Shelf Research 18, 805–829.

Hoffmann, L.J., Peeken, I., Lochte, K., Assmy, P., Veldhuis, M., 2006. Different reactions of Southern Ocean phytoplankton size classes to iron fertilization. Limnology and Oceanography 51, 1217–1229.

Holeton, C.L., Nedelec, F., Sanders, R., Brown, L., Moore, C.M., Stevens, D.P., Heywood, K.J., Statham, P.J., Lucas, C.H., 2005. Physiological state of phytoplankton communities in the Southwest Atlantic sector of the Southern Ocean, as measured by fast repetition rate fluorometry. Polar Biology 29, 44–52.

Johnson, K.S., Karl, D.M., 2002. Is ocean fertilization credible and creditable? Science 296, 467–468.

Joos, F., Sarmiento, J.L., Siegenthaler, U., 1991. Estimates of the effect of Southern Ocean iron fertilization on atmospheric CO2 concentrations. Nature 349, 772–775.

Kaufman, A., Li, Y.-H., Turekian, K.K., 1981. The removal rates of $^{234}$Th and $^{228}$Th from waters of the New York Bight. Earth and Planetary Science Letters 54, 385–392.

Korb, R.E., Whitehouse, M., 2004. Contrasting primary production regimes around South Georgia, Southern Ocean: large blooms versus high nutrient, low chlorophyll waters. Deep-Sea Research I 51, 721–738.

Ku, T.-L., Knauss, K.G., Mathieu, G.G., 1977. Uranium in the open ocean: concentration and isotopic composition. Deep-Sea Research 24, 1005–1017.

Lam, P.J., Bishop, J.K.B., 2007. High biomass low export regimes in the Southern Ocean. Deep-Sea Research II 54, 601–638.

Law, C.S., Abraham, E.R., Watson, A.J., Liddicoat, M.I., 2003. Vertical eddy diffusion and nutrient supply to the surface mixed layer of the Antarctic Circumpolar Current. Journal of Geophysical Research 108 [doi:10.1029/2002JC001604].

Lucas, M., Seeyave, S., Sanders, R., Moore, C.M., Williamson, R., Stinchcombe, M., 2007. Nitrogen uptake responses to a naturally Fe-fertilised phytoplankton bloom during the 2004/5 CROZEX study. Deep-Sea Research II, in press, doi:10.1016/j.dsr2.2007.06.017.

Martin, J.H., 1990. Glacial-interglacial $CO_2$ change: the iron hypothesis. Paleoceanography 5, 1–13.

Martin, J.H., Gordon, R.M., Fitzwater, S.E., 1990. Iron in Antarctic waters. Nature 345, 156–158.

Martin, J.H., Coale, K.H., Johnson, K.S., Fitzwater, S.E., Gordon, R.M., Tanner, S.J., Hunter, C.N., Elrod, V.A., Nowicki, J.L., Coley, T.L., Barber, R.T., Lindley, S., Watson, A.J., Vanscoy, K., Law, C.S., Liddicoat, M.I., Ling, R., Stanton, T., Stockel, J., Collins, C., Anderson, A., Bidigare, R., Ondrusek, M., Latasa, M., Millero, F.J., Lee, K., Yao, W., Zhang, J.Z., Friederich, G., Sakamoto, C., Chavez, F., Buck, K., Kolber, Z., Greene, R., Falkowski, P., Chisholm, S.W., Hoge, F., Swift, R., Yungel, J., Turner, S., Nightingale, P., Hatton, A., Liss, P., Tindale, N.W., 1994. Testing the iron hypothesis in ecosystems of the equatorial Pacific Ocean. Nature 371, 123–129.

Metzl, N., Tilbrook, B., Poisson, A., 1999. The annual $fCO_2$ cycle and the air-sea $CO_2$ flux in the sub-Antarctic Ocean. Tellus 51B, 849–861.

Moore, W.S., 2000. Determining coastal mixing rates using radium isotopes. Continental Shelf Research 20, 1993–2007.

Moran, S.B., Buesseler, K.O., 1993. Size-fractionated $^{234}$Th in continental shelf waters off New England: implications for the

role of colloids in oceanic trace metal scavenging. Journal of Marine Research 51, 893–922.

Naveira Garabato, A.C., Polzin, K.L., King, B.A., Heywood, K.J., Visbeck, M., 2004. Widespread intense turbulent mixing in the Southern Ocean. Science 303, 210–213.

Nodder, S.D., Charette, M.A., Waite, A.M., Trull, T.W., Boyd, P.W., Zeldis, J., Buesseler, K.O., 2001. Particle transformations and export flux during an *in situ* iron-stimulated algal bloom in the Southern Ocean. Geophysical Research Letters 28, 2409–2412.

Planquette, H., Statham, P.J., Fones, G.R., Charette, M.A., Moore, M., Salter, I., Nédélec, F.H., Taylor, S.L., French, M., Baker, A.R., Mahowald, N., Jickells, T.D., 2007. Dissolved iron in the vicinity of the Crozet Islands, Southern Ocean. Deep-Sea Research II, in press, doi:10.1016/j.dsr2.2007.06.019.

Pollard, R.T., Read, J.F., 2001. Circulation pathways and transports of the Southern Ocean in the vicinity of the Southwest Indian Ridge. Journal of Geophysical Research 106, 2881–2898.

Pollard, R. T., Sanders, R., 2006. RRS *Discovery* cruises 285/286, 3 Nov-10 Dec 2004, 13 Dec 2004–21 Jan 2005; CROZet circulation, iron fertilization and EXport production experiment (CROZEX). Southampton Oceanography Centre, Cruise Report No. 60.

Pollard, R.T., Lucas, M.I., Read, J.F., 2002. Physical controls on biogeochemical zonation in the Southern Ocean. Deep-Sea Research II 49, 3289–3305.

Pollard, R.T., Sanders, R., Lucas, M.I., Statham, P.J., 2007a. The Crozet natural iron bloom and EXport experiment (CROZEX). Deep-Sea Research II, in press, doi:10.1016/j.dsr2.2007.07.023.

Pollard, R.T., Venables, H.J., Read, J.F., Allen, J.T., 2007. Large-scale circulation around the Crozet Plateau controls an annual phytoplankton bloom in the Crozet Basin. Deep-Sea Research II, in press, doi:10.1016/j.dsr2.2007.06.012.

Prentice, I.C., Farquhar, G.D., Fasham, M.J.R., Goulden, M.L., Heimann, M., Jaramillo, V.J., Kheshgi, H.S., Le Quéré, C., Scholes, R.J., Wallace, D.W.R., 2001. The carbon cycle and atmospheric carbon dioxide, chapter 3. In: Houghton, J.T., Ding, Y., Griggs, D.J., Noguer, M., van der Linden, P.J., Dai, X., Maskell, K., Johnson, C.A. (Eds.), Climate Change 2001: The Scientific Basis. Contributions of Working Group I to the Third Assessment Report of the International Panel on Climate Change. Cambridge University Press, Cambridge.

Rutgers van der Loeff, M., Vöge, I., 2001. Does Fe fertilisation enhance the export production as measured through the $^{234}Th/^{238}U$ disequilibrium in surface water? In: Smetacek, V., Bathmann, U., El Naggar, S. (Eds.), The expeditions ANTARKTIS XVIII/1-2 of the Research Vessel Polarstern in 2000. Berichte zur Polar- und Meeresforschnung (Reports on Polar and Marine Research) 400, AWI, Bremerhaven, Germany, pp. 222–225.

Rutgers van der Loeff, M.M., Moore, W.S., 1999. Determination of natural radioactive tracers. In: Grasshoff, K., Kremling, K., Ehrhardt, M. (Eds.), Methods of Seawater Analysis. Wiley-VCH, Weinheim (Chapter 13).

Rutgers van der Loeff, M.M., Friedrich, J., Bathmann, U.V., 1997. Carbon export during the Spring Bloom at the Antarctic Polar Front, determined with the natural tracer $^{234}Th$. Deep-Sea Research II 44, 457–478.

Rutgers van der Loeff, M.M., Buesseler, K., Bathmann, U., Hense, I., Andrews, J., 2002. Comparison of carbon and opal export rates between summer and spring bloom periods in the region of the Antarctic Polar Front, SE Atlantic. Deep-Sea Research II 49, 3849–3869.

Rutgers van der Loeff, M., Sarin, M.M., Baskaran, M., Benitez-Nelson, C., Buesseler, K.O., Charette, M., Dai, M., Gustafsson, Ö., Masque, P., Morris, P.J., Orlandini, K., Rodriguez y Baena, A., Savoye, N., Schmidt, S., Turnewitsch, R., Vöge, I., Waples, J., 2006. A review of present techniques and methodological advances in analyzing $^{234}Th$ in aquatic systems. Marine Chemistry 100, 190–212.

Salter, I., Lampitt, R.S., Sanders, R., Poulton, A., Kemp, A.E.S., Boorman, B., Saw, K., Pearce, R., 2007. Estimating carbon, silica and diatom export from a naturally fertilised phytoplankton bloom in the Southern Ocean using PELAGRA: a novel drifting sediment trap. Deep-Sea Research II, in press, doi:10.1016/j.dsr2.2007.06.008.

Sanders, R., Jickells, T., 2000. Total organic nutrients in Drake Passage. Deep-Sea Research I 47, 997–1014.

Sanders, R., Brown, L., Henson, S., Lucas, M., 2005. New production in the Irminger Basin during 2002. Journal of Marine Systems 55, 291–310.

Sanders, R., Morris, P.J., Stinchcombe, M., Seeyave, S., Venables, H., Lucas, M., Moore, M., 2007. New production and the *f*-ratio around the Crozet Plateau in austral summer 2004–5 diagnosed from seasonal changes in inorganic nutrient levels. Deep-Sea Research II, in press, doi:10.1016/j.dsr2.2007.06.007.

Santschi, P.H., Li, Y.-H., Bell, J., 1979. Natural radionuclides in the water of Narragansett Bay. Earth and Planetary Science Letters 45, 201–213.

Sarmiento, J.L., Orr, J.C., 1991. Three-dimensional simulations of the impact of Southern Ocean nutrient depletion on atmospheric $CO_2$ and ocean chemistry. Limnology and Oceanography 36, 1928–1950.

Savoye, N., Benitez-Nelson, C., Burd, A.B., Cochran, J.K., Charette, M., Buesseler, K.O., Jackson, G.A., Roy-Barman, M., Schmidt, S., Elskens, M., 2006. $^{234}Th$ sorption and export models in the water column: a review. Marine Chemisrty 100, 234–249.

Savoye, N., Trull, T.W., Jacquet, S.H.M., Navez, J., Dehairs, F., 2007. $^{234}Th$-based export fluxes during a natural iron fertilization experiment in the Southern Ocean (KEOPS). Deep-Sea Research II, KEOPS issue.

Seeyave, S., Lucas, M.I., Moore, C.M., Poulton, A.J., 2007. Phytoplankton productivity and community structure in the vicinity of the Crozet Plateau during austral summer 2004/2005. Deep-Sea Research II, in press, doi:10.1016/j.dsr2.2007.06.010.

Speicher, E.A., Moran, S.B., Burd, A.B., Delfanti, R., Kaberi, H., Kelly, R.P., Papucci, C., Smith, J.N., Stavrakakis, S., Torricelli, L., Zervakis, V., 2006. Particulate organic carbon export fluxes and size-fractionated $POC/^{234}Th$ ratios in the Ligurian, Tyrrhenian and Aegean Seas. Deep-Sea Research I 53, 1810–1830.

Tanaka, N., Takeda, Y., Tsunogai, S., 1983. Biological effect on removal of Th-234, Po-210 and Pb-210 from surface water in Funka Bay, Japan. Geochemica Cosmochemica Acta 47, 1783–1790.

Thomalla, S., Turnewitsch, R., Lucas, M., Poulton, A., 2006. Particulate organic carbon export from the North and South

Atlantic gyres: the $^{234}Th/^{238}U$ disequilibrium approach. Deep-Sea Research II 53, 1629–1648.

Tsuda, A., Takeda, S., Saito, H., Nishioka, J., Nojiri, Y., Kudo, I., Kiyosawa, H., Shiomoto, A., Imai, K., Ono, T., Shimamoto, A., Tsumune, D., Yoshimura, T., Aono, T., Hinuma, A., Kinugasa, M., Suzuki, K., Sohrin, Y., Noiri, Y., Tani, H., Deguchi, Y., Tsurushima, N., Ogawa, H., Fukami, K., Kuma, K., Saino, T., 2003. A mesoscale iron enrichment in the Western Subarctic Pacific induces a large centric diatom bloom. Science 300, 958–961.

Tsunogai, S., Minagawa, M., 1976. Vertical Flux of Organic Materials Estimated from Th-234 in the Oceans. Joint Oceanographic Assembly, Edinburgh.

Tsunogai, S., Taguchi, K., Harada, K., 1986. Seasonal variation in the difference between observed and calculated particulate fluxes of Th-234 in Funka Bay, Japan. Journal of the Oceanographical Society of Japan 42, 91–98.

Turnewitsch, R., Springer, B.M., 2001. Do bottom mixed layers influence $^{234}Th$ dynamics in the abyssal near-bottom water column? Deep-Sea Research I 48, 1279–1307.

Venables, H.J., Pollard, R.T., Popova, E.E., 2007. Physical conditions controlling the early development of a regular phytoplankton bloom north of the Crozet Plateau, Southern Ocean, described using remotely sensed data. Deep Sea Research II, in press, doi:10.1016/j.dsr2.2007.06.014.

Vöge, I., Savoye, N., Berg, G.M., Bertoïa, C., Klaas, C., Bathmann, U., Strass, V., Friedrich, J., Dehairs, F., 2006. 234Th-based export production during the European Iron Fertilization Experiment (EIFEX) Ocean Sciences Meeting, Honolulu, Hawaii, OS35M-17.

Waples, J.T., Benitez-Nelson, C., Savoye, N., Rutgers van der Loeff, M., Baskaran, M., Gustafsson, Ö., 2006. An introduction to the application and future use of $^{234}Th$ in aquatic systems. Marine Chemistry 100, 166–189.

Wei, C.-L., Murray, J.W., 1991. $^{234}Th/^{238}U$ disequilibria in the Black Sea. Deep-Sea Research I 38, S855–S873.

Zeebe, R.E., Archer, D., 2005. Feasibility of ocean fertilization and its impact on future atmospheric $CO_2$ levels. Geophysical Research Letters 32, L09703, doi:10.1029/2005GL022449.

Zeebe, R.E., Archer, D., 2006. Is large scale iron fertilization a feasible strategy to sequester anthropogenic $CO_2$. Eos, Transactions, AGU, 87(36), Ocean Sciences Meeting Supplemental, Abstract OS34F.